СООБЩЕНИЯ
ОБЪЕДИНЕННОГО
ИНСТИТУТА
ЯДЕРНЫХ
ИССЛЕДОВАНИЙ
ДУБНА

E2 - 11222

H.Dorn, D.Ebert, V.N.Pervushin

QUARK SEA CONTRIBUTIONS TO DEEP INELASTIC SCATTERING IN TWO-DIMENSIONAL QCD

1978

E2 - 11222

H.Dorn, D.Ebert, V.N.Pervushin

QUARK SEA CONTRIBUTIONS TO DEEP INELASTIC SCATTERING IN TWO-DIMENSIONAL QCD

Дорн Х., Эберт Д., Первушин В.Н. Е2 - 11222

Вклад кварков из моря (sea–quarks) в глубоконеупругое рассеяние в двумерной К.Х.Д.

В рамках двумерной квантовой хромодинамики в бъеркеновском пределе найден вклад невалентных кварков (sea–quarks) в структурную функцию глубоконеупругого рассеяния. При больших N рассматриваются "цилиндрические" диаграммы, вклад которых интерпретируется как перенормировка вычета f -траектории с квантовыми числами вакуума.

Работа выполнена в Лаборатории теоретической физики ОИЯИ.

Сообщение Объединенного института ядерных исследований. Дубна 1978

Dorn H., Ebert D., Pervushin V.N. E2 - 11222

Quark Sea Contributions to Deep Inelastic Scattering in Two-Dimensional QCD

Quark sea contributions to the partition function are studied in the Bjorken limit using two-dimensional QCD in the 1/N approximation. The cylinder graphs considered yield a contribution which is associated to "residuum renormalization" of the "f" - trajectory exchanged in the vacuum channel.

The investigation has been performed at the Laboratory of Theoretical Physics, JINR.

Communication of the Joint Institute for Nuclear Research. Dubna 1978

1. INTRODUCTION

QCD, the non-Abelian gauge theory of coloured quarks and gluons, is at present the most prominent candidate for a theory describing the hadronic world. This rests mainly on the property of asymptotic freedom and the possibility that the infrared instability of QCD confines the quarks [1]. Despite many attempts quark confinement has, however, not yet been proved for four-dimensional QCD. In this situation it is of importance that two-dimensional QCD (QCD_2) can be solved in leading order of an $1/N$ expansion, where N is the number of colours, yielding an infinite number of bound state mesons as well as confinement of quarks and gluons [2]. A transparent formulation of QCD_2 in terms of bound state fields may further be obtained by using functional methods [3]. Moreover, there exists an extensive literature [4,5] on the Regge asymptotic behaviour of scattering amplitudes for this model. Although confinement is almost trivial in two dimensions, a merit of QCD_2 is to provide us with an example of how final bound state hadrons in deep inelastic scattering realize Bjorken scaling in a way demanded by the asymptotic freedom of the theory. Einhorn [6] has evaluated the Bjorken limit of the graphs shown in *fig. 1* which yield the leading order contribution to deep inelastic scattering by the valence quarks inside the mesons. The quark partition function is in this case determined by the square of the meson bound state wave function. There is, however, an additional possibility for a virtual photon to scatter with quark-antiquark pairs $c\bar{c}$ created by gluons out of the quark sea. It is of importance to study such effects in order to understand the consequences of the sea and to check whether the dynamical picture of hadrons is self-consistent.

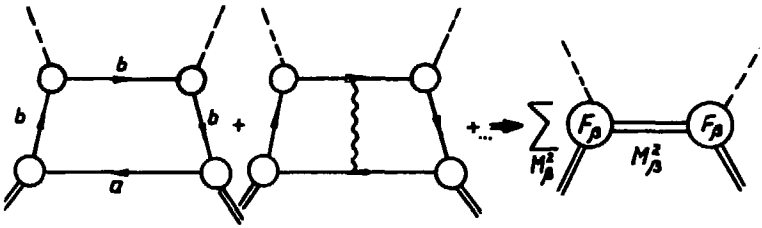

Fig. 1. Inelastic scattering by valence quarks as the square of form factors[6].

In this paper we shall investigate a contribution of sea quarks to the structure function of deep inelastic scattering in QCD_2. For simplicity, we shall consider the correction terms of an order of $1/N$ containing only one $c\bar{c}$ -loop which are depicted in *fig. 2a*. This class of diagrams is particularly interesting because the graphs possess the topology of the bare Pomeron of the dual model [7] (cf. *fig. 2b*). The paper is organized as follows. In Sec. 2 we derive the formula of the quark sea contributions to the virtual Compton amplitude. Section 3 is devoted to the study of the Bjorken limit including a detailed investigation of different regions of the phase space. Section 4 contains a summary of the results. There are two appendices presenting some formulas and results that are needed in the text.

2. *DEEP INELASTIC SCATTERING*

We shall consider quantum chromodynamics in two-dimensions (QCD_2) which was investigated in the limit $N \to \infty$, g^2N fix, in leading order of $1/N$ in the light-cone gauge[2], where g is the gauge coupling constant and N the number of colours (for the Feynman rules,

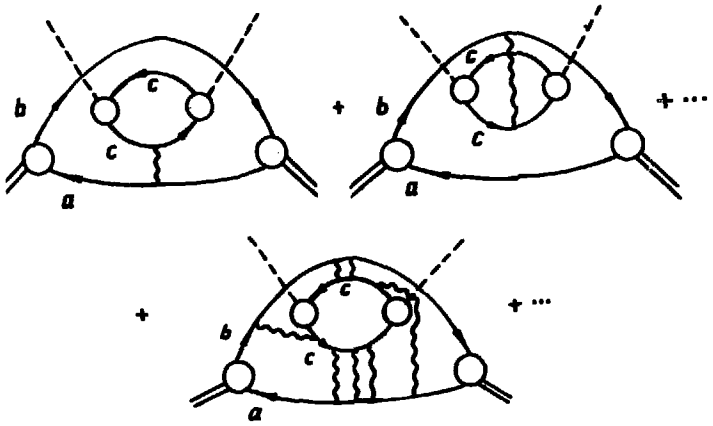

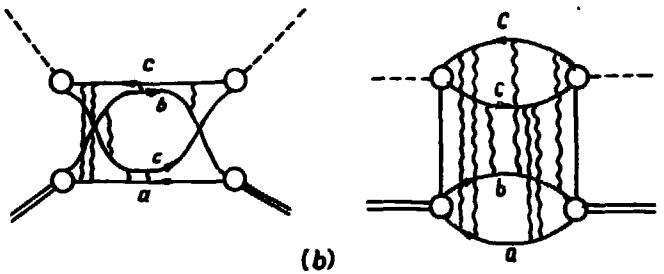

Fig. 2. a) Inelastic scattering by a pair $c\bar{c}$ *of sea quarks. b) Equivalent representation of a process with sea quarks as a twisted loop or cylinder graph with gluonic exchange, respectively.*

see app. A). The two-dimensional analogue of the deep inelastic scattering $eM \to eX$ of an electron by a bound state meson M of momentum p is described by the Bjorken limit of the tensor $W_{\mu\nu} = \int d^2x e^{iqx} \langle M,p|j_\mu(x)j_\nu(0)|M,p\rangle$, which is the discontinuity of the corresponding virtual Compton amplitude in the variable $s=(p+q)^2$. $W_{\mu\nu}$ may be expressed by the structure function $W(q^2,\nu)$ *

$$W_{\mu\nu} = (p_\mu - \frac{q_\mu \nu}{q^2})(p_\nu - \frac{q_\nu \nu}{q^2}) W(q^2, \nu), \qquad (1)$$

where, as usual, we define

$$\nu = p \cdot q, \quad x_{Bj} = \frac{-q^2}{2\nu}; \quad p^2 = M^2.$$

The scattering of a virtual photon with the valence quarks b and $\bar{a}$ forming the bound state meson M (cf. *fig. 1*) has been studied in leading order of the 1/N expansion by Einhorn /6/. Its contribution is just given by the square of the meson form factor summed over all intermediate meson resonances. A virtual photon may, however, also scatter with a quark-antiquark pair $c\bar{c}$ created by gluons out of the quark sea. In the following we shall investigate the contribution of such sea quarks to $W_{\mu\nu}$ restricting ourselves, for simplicity, to the graphs of *fig. 2a* containing only one $c\bar{c}$-loop. We may redraw these graphs in the form of a twisted loop or cylinder graph with two quark boundaries and no handles (cf. *fig. 2b*). Thus, it becomes evident that the set of graphs considered possesses just the topology of the bare Pomeron of the dual model /7/. Calculating the discontinuity of the above graphs quark singularities should cancel as usual, because of confinement, so that intermediate bound state mesons contribute alone. Hence, we have to consider only the discontinuity of the graph shown in *fig. 3a* and to sum over the intermediate mesons. Let us denote the ampli-

---

* In QCD_2 there exists only one independent structure function owing to the relation ($q^2 < 0$)

$$p_\mu = \frac{\nu}{q^2} q_\mu + \frac{\sqrt{\nu^2 - q^2 M^2}}{q^2} \epsilon_{\mu\sigma} q^\sigma \operatorname{sgn} q_1 .$$

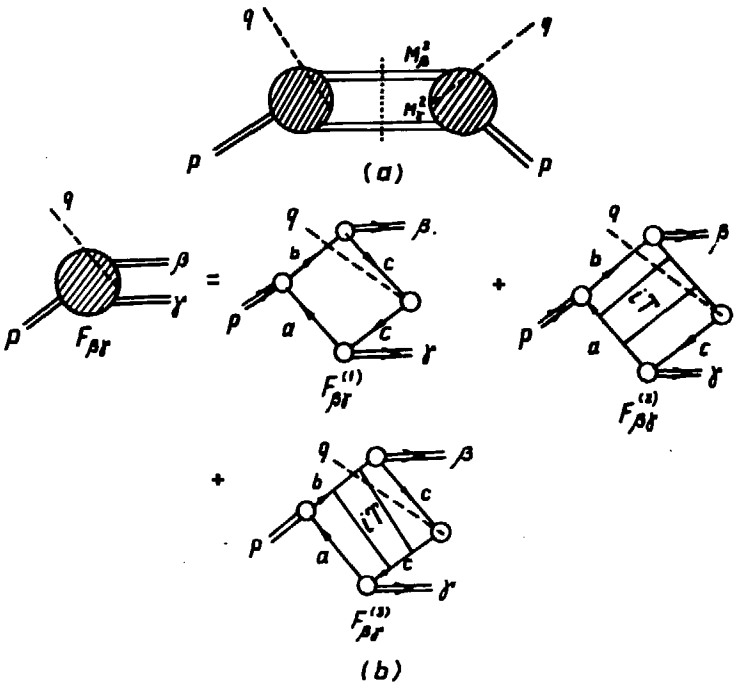

Fig. 3. a) The absorptive part of the virtual Compton amplitude with two intermediate mesonic states. b) The amplitude $F_{\beta\gamma}$ *to leading order in* $1/N$.

tude drawn in *fig. 3b* by $F_{\beta\gamma}(pq;p_\beta p_\gamma)$. T is the quark-antiquark scattering amplitude. It is simplest to calculate W_{--} which is given by

$$W_{--} = \sum_{\beta,\gamma} \int \frac{d^2k}{(2\pi)^2} |F_{\beta\gamma}(pq;p+q-k,k)|^2 \delta_+(k^2-M_\gamma^2) \times$$

$$\times \delta_+((p+q-k)^2-M_\beta^2). \qquad (2)$$

Performing the integration, we get

$$W_{--} = \frac{1}{8\pi^2} \sum_{\beta,\gamma} \int_{(M_\beta+M_\gamma)^2<(p+q)^2} \lambda^{-1/2}(s, M_\beta^2, M_\gamma^2) \sum_{i=\pm} |F_{\beta\gamma}(pq; p_\beta^{(i)} p_\gamma^{(i)})|^2, \tag{3}$$

where λ is the usual triangular function and

$$p_{\gamma-}^{(\pm)} = \frac{s+M_\gamma^2-M_\beta^2 \mp \lambda^{1/2}(s, M_\beta^2, M_\gamma^2)}{4(p_+ + q_+)},$$

$$p_{\beta-}^{(\pm)} = \frac{s+M_\beta^2-M_\gamma^2 \pm \lambda^{1/2}(s, M_\beta^2, M_\gamma^2)}{4(p_+ + q_+)}, \tag{4}$$

$$p_\pm = \frac{1}{\sqrt{2}}(p_0 \pm p_1); \quad s = (p+q)^2, \quad p_\beta^2 = M_\beta^2, \text{etc.}$$

The two upper signs $\pm$ of the momenta (4) correspond to whether the mesons β, γ are right-moving or left-moving.

2.1. Kinematics in Einhorn's Reference Frame

We consider a system, where $q_- < 0$, q_- fix (q ingoing). Defining $x = -\frac{q_-}{p_-}$ we find the following relations in the Bjorken limit $\nu(s) \to \infty$, $q^2 \to -\infty$, x_{Bj} fixed,

$$x_{Bj} = x + O(\frac{1}{s}),$$

$$q^2 = -s\frac{x}{1-x} + O(1); \quad \nu = \frac{s}{2(1-x)} + O(1), \tag{5}$$

$$p_- + q_- = p_-(1-x); \quad p_+ + q_+ = \frac{s}{2p_-(1-x)}.$$

For further reference, we list also some ordering relations between different "-" components of momenta involved. Since p , p_γ , p_β are the momenta of ingoing or outgoing particles, we have

$$p_- , p_{\gamma -} , p_{\beta -} > 0 .$$

Together with $q_- < 0$ and momentum conservation, this yields

$$p_- - p_{\beta -} = p_{\gamma -} - q_- > 0 , \quad p_- - p_{\gamma -} = p_{\beta -} - q_- > 0 . \tag{6}$$

2.2. *The Amplitude* $F_{\beta\gamma}$

The diagrams of *fig. 3b* can now be calculated using the expressions for the quark propagator, the T -matrix, the vertex function and the quark formfactor of ref. [6] (see also appendix A). Let us consider, for example, the diagram $F^{(2)}_{\beta\gamma}$. We get

$$F^{(2)}_{\beta\gamma} = -2ie_c N^2 \int \frac{d^2k}{(2\pi)^2} \int \frac{d^2\ell}{(2\pi)^2} S_c(k-q) Q^{c\bar{c}}(k,q) S_c(k) \times$$

$$\times \Gamma^{c\bar{a}}(k, p_\gamma) S_a(k - p_\gamma) \cdot iT(k - p_\gamma, \ell - p; (q - p_\gamma)^2) S_a(\ell - p) \times$$

$$\times \Gamma^{b\bar{a}}(\ell, p) S_b(\ell) \Gamma^{b\bar{c}}(\ell, p_\beta) S_c(\ell - p_\beta) . \tag{7}$$

As only the quark propagators depend on the "+" components of the momenta, the respective loop integration over k_+ , ℓ_+ can easily be done. In the case of three quark propagators we obtain, e.g.,

$$\int dk_+ S_i(k_i) S_j(k_j) S_\ell(k_\ell) =$$

$$= \pi \{ \Theta(-k_{i-}) \Theta(k_{j-}) \Theta(k_{\ell-}) - \Theta(k_{i-}) \Theta(-k_{j-}) \Theta(-k_{\ell-}) \} h(i,j) h(i,\ell)$$

$$+ \{ \Theta(k_{i-}) \Theta(-k_{j-}) \Theta(k_{\ell-}) - \Theta(-k_{i-}) \Theta(k_{j-}) \Theta(-k_{\ell-}) \} h(j,i) h(j,\ell)$$

$$+\{\Theta(k_{i_-})\Theta(k_{j_-})\Theta(-k_{\ell_-}) - \Theta(-k_{i_-})\Theta(-k_{j_-})\Theta(k_{\ell_-})\}\,h(\ell,i)h(\ell,j)], \tag{8}$$

where

$$h(i,j) = \frac{(k_i - k_j)_-}{\frac{m_i^2 - m^2}{k_{i_-}/(k_i - k_j)_-} - \frac{m_j^2 - m^2}{k_{j_-}/(k_i - k_j)_-} - (k_i - k_j)^2} = -h(j,i),$$

$$m^2 = \frac{g^2 N}{\pi}. \tag{9}$$

A similar formula holds in the case of four internal propagators. The single terms in the r.h.s. of eq. (8) can be visualized graphically by x_- – "time" ordered graphs [4,6] where quark lines are directed to the right (left) if their momentum k_- is positive (negative). This rule may be extended to the momenta of the bound states and the current, too. In most of such ordered graphs the above factors h may be absorbed by the vertex function, the quark form factor or the T-matrix, respectively, [4] (see eqs. (A3, A6, A8) of App. A). Applying eq.(8) to eq. (7) and using eqs. (A.3), (A.6) in a way to cancel as many h's as possible, we arrive at the graphs of *fig.4d-i*. These graphs are to be understood with the following modified rules:

gluon line: $\frac{1}{k_-^2}$

quark line: 1 (10)

gluon-quark vertex: 1

meson wave functions: $\Phi_n^{a\bar{b}}(k_-/p_{n-})$.

Note that there appear gluon propagators in the diagrams because we have used eq. (A.2) in order to "turn" around a quark with $x = \frac{k_-}{p_-} < 0$ at a vertex into a quark with

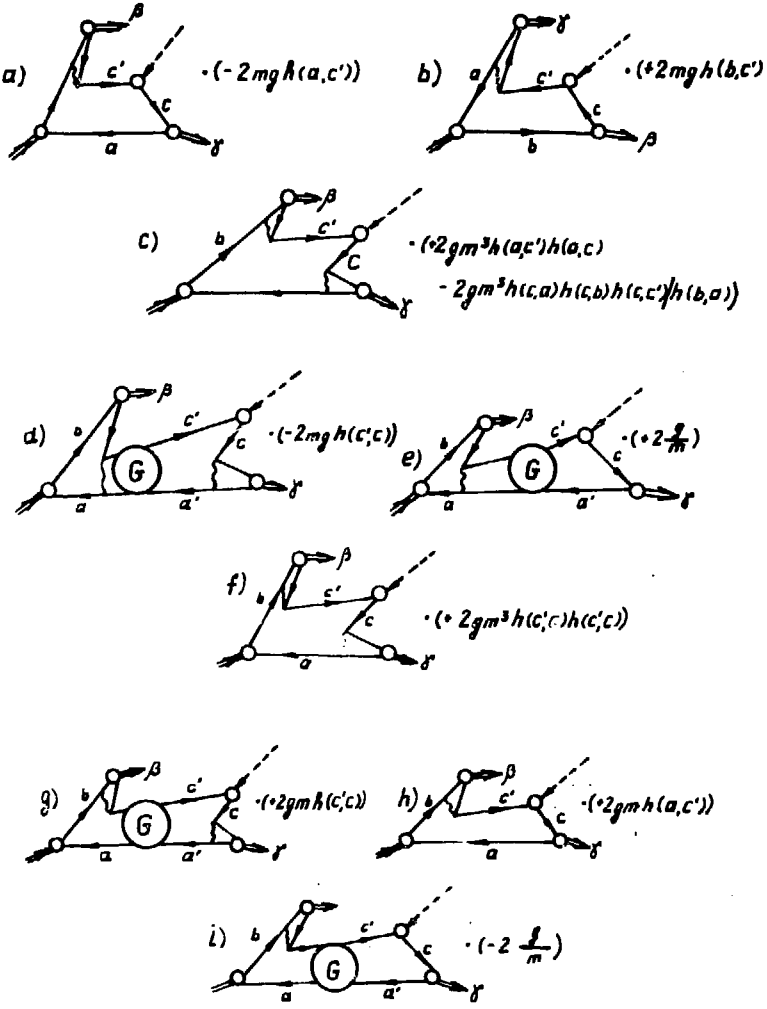

Fig. 4. a)-i). "Time" ordered perturbation theoretical diagrams contributing to $F_{\beta\gamma}^{(1)}$ *(a-c) and to* $F_{\beta\gamma}^{(2)}$ *(d-i). (Momenta* k_c, k_c' *of c-quarks are denoted by* c, c' *etc.).*

$0 \leq x \leq 1$. The quark form factor is yet unchanged. All remaining factors are written down explicitly as a number multiplying the expression of the corresponding graph obtained by means of (10). The ordered graphs belonging to the contributions $F^{(1)}_{\beta\gamma}$, $F^{(3)}_{\beta\gamma}$ of *fig. 3* may be derived analogously. The graphs of $F^{(1)}_{\beta\gamma}$ are depicted in *fig. 4a-c*. Finally, the graphs belonging to $F^{(3)}_{\beta\gamma}$ may be obtained from those of $F^{(2)}_{\beta\gamma}$ by replacing $\beta \to \gamma$ and reversing the direction of the quark lines. Now *4a)* cancels *4h)*, and *4b)* cancels the analogous graph of $F^{(3)}_{\beta\gamma}$. The remaining 11 ordered graphs can be collected into three groups if we use the concepts of the three-meson vertex /2,4/, the meson form factor /6/ and an irreducible four-point coupling between a current and three mesons. The graphs *4d), e), g), i)* and their analogs of $F^{(3)}_{\beta\gamma}$ are represented by the second and third diagrams of *fig. 5*, respectively. The remaining graphs *4c), f)* and an analogous graph from $F^{(3)}_{\beta\gamma}$ constitute the irreducible four-point coupling which by the algebraic identity

$$\left(h(a,c')h(a,c) - \frac{h(c,a)h(c,b)h(c,c')}{h(b,a)}\right) + h(c',a)h(c',c) + h(c',b)h(c',c) = 0. \tag{11}$$

is identically zero. In the next step we use eq. (A.8) to

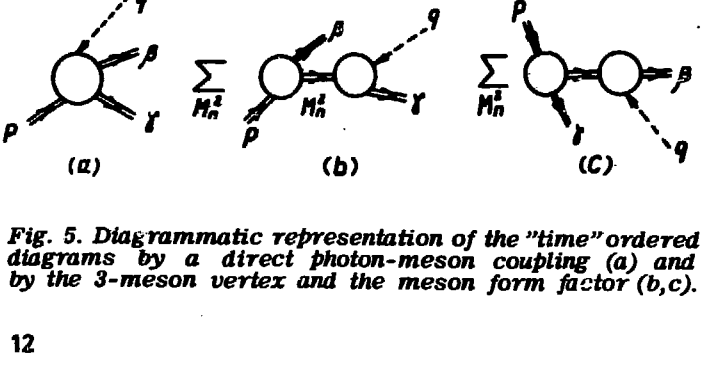

Fig. 5. Diagrammatic representation of the "time" ordered diagrams by a direct photon-meson coupling (a) and by the 3-meson vertex and the meson form factor (b,c).

eliminate the last h -factors. After some substitutions in the integrals involved we, finally, arrive at

$$F_{\beta\gamma}(p,q;p_\beta p_\gamma)=F_{\underline{\beta}\gamma}(\dots)+F_{\beta\underline{\gamma}}(\dots) \tag{12}$$

$$F_{\underline{\beta}\gamma}(p,q;p_\beta p_\gamma)=\frac{4ig\eta p_{\gamma-}c_c}{m}\int_0^1 dydzdy'dz'\times$$

$$\times\frac{\Phi_{M^2}^{b\bar{a}}\left(\frac{1+z\eta}{1+\eta}\right)-\Phi_{M^2}^{b\bar{a}}\left(\frac{1-y}{1+\eta}\right)}{(y+z\eta)^2}\times\Phi_{M_\beta^2}^{b\bar{c}}(1-y)\Phi_{M_\gamma^2}^{c\bar{a}}(z')\times$$

$$\times\{G^{c\bar{a}}\left(z,\frac{1+z'\eta'}{1+\eta'};\frac{(p_\gamma-q)^2}{m^2}\right)-$$

$$-\frac{G^{c\bar{c}}\left(1-y';\frac{q^2}{m^2}\right)}{(y'+z'\eta')^2}\left[G^{c\bar{a}}\left(z,\frac{1+z'\eta'}{1+\eta'};\frac{(p_\gamma-q)^2}{m^2}\right)-G^{c\bar{a}}\left(z,\frac{1-y'}{1+\eta'};\frac{(p_\gamma-q)^2}{m^2}\right)\right]\}, \tag{13}$$

$$\eta=\frac{(p-p_\beta)_-}{p_{\beta-}},\quad \eta'=-\frac{p_{\gamma-}}{q_-},$$

where the Green functions $G(x,y;p^2)$, $G(x;p^2)$ are defined in the appendix, and we have written $\Phi_{M_n^2}$ instead of Φ_n ($M_n^2\sim\pi^2m^2n$). The above expression $F_{\beta\gamma}$ represents the graphs *4d), e), g), i)* = second graph of *fig. 5*. $F_{\beta\underline{\gamma}}$ corresponds to the third graph of *fig. 5* and may be obtained from (13) by the change $\beta\leftrightarrow\gamma$ and a suitable change of the flavour indices. We mention that the above ordered graph scheme depends on the reference frame and the kinematical region under consideration.

3. *ASYMPTOTIC BEHAVIOUR OF* $F_{\beta\gamma}$ *IN THE BJORKEN LIMIT*

In the following we shall compute the contribution of the above graphs to the partition function $f(x)$ for deep inelastic scattering by sea quarks *

$$f(x) = \lim_{Bj} \nu^2 W(q^2, \nu). \tag{14}$$

Before estimating different contributions of the phase space to the sum in eq. (3), let us recall briefly the results obtained for the *Regge limit* of the cylinder graph with external mesons only [4,5]. As has been found, the phase space region M_β^2 , $M_\gamma^2 = O(1)$ yields a Regge-Regge cut contribution. From the region $M_\beta^2 = O(s)$, $M_\gamma^2 = O(s)$ each of the ordered diagrams gets an asymptotic contribution reminiscent of Pomeron exchange. There works, however, in the Regge limit an intriguing cancellation between different asymptotic contributions so that really no net bare Pomeron in QCD_2 does appear. Finally, the regions $M_\beta^2 = O(s)$, M_γ^2 fix (M_β^2 fix, $M_\gamma^2 = O(s)$) and $M_\beta^2, M_\gamma^2 = O(\sqrt{s})$ lead to a residuum or trajectory renormalization of the ordinary "f"-trajectory, respectively, that breaks exchange degeneracy.

Let us now evaluate the contribution of the analogous phase space regions to deep inelastic scattering and ask whether a cancellation mechanism works also in the Bjorken limit of the cylinder graph with external currents. This question is not trivially answered because the cancellation may be incomplete for processes with external currents [8]. Moreover, there contribute other sets of or-

---

* Using dimensional counting arguments one should take into consideration that in QCD_2 coupling constants have a mass dimension $[g;e] = 1$. With $[\langle M, p \rangle] = 1$, $[j_\mu]$ (including e_c) $= 2$ we find $[W_{\_\_}] = 2$ and $[W] = 0$. The partition function contains then a dimensional factor (comp. eq. 26).

dered diagrams in the Bjorken region ($q_- < 0$) than in the Regge region ($q_- > 0$).

i). $M_\beta^2, M_\gamma^2 = O(1)$

We start with the discussion of $F_{\beta\gamma}$. The relevant kinematics following from eqs. (4), (5) has been grouped together in the *Table*. Using eqs. (B9,B12) we find

$$F_{\beta\gamma}(pq;p_\beta^{(+)}p_\gamma^{(+)}) = \frac{4igxp_-e_c}{m}\left(\frac{M_\gamma^2}{s}\right)^{1+\beta_a} \times$$

$$\times\left(\frac{1-x}{x}\right)^{\beta_a}\int_0^1 dydzdz' \frac{\Phi_{M^2}^{b\bar{a}}(1-x+zx) - \Phi_{M^2}^{b\bar{a}}((1-y)(1-x))}{\left(y+z\frac{x}{1-x}\right)^2} \times$$

$$\times\Phi_{M_\beta^2}^{b\bar{c}}(1-y)\Phi_{M_\gamma^2}^{c\bar{a}}(z')(1-z')^{\beta_a}\hat{C}^{a\bar{c}}\left(z, M^2x - M_\beta^2\frac{x}{1-x}\right) + O\left(\frac{1}{s^{1+\beta_a}}\right) =$$

$$= O\left(\frac{1}{s}\right). \qquad (15)$$

For illustration, we have written down in eq. (15) the contribution from the direct coupling of the current. In a similar manner one proves $F_{\beta\gamma}(pq;p_\beta^{(-)}p_\gamma^{(-)}) = O\left(\frac{1}{s}\right)$. Further, taking into account $\lambda^{-1/2}(s, M_\beta^2, M_\gamma^2) \sim 1/s$, we get $W^{(i)}(q^2,\nu) = O(1/s^3)$. Thus, there is no contribution to the partition function $f(x)$.

ii). $M_\beta^2 = \beta^2 s, M_\gamma^2 = \gamma^2 s$

Now for fixed β, γ masses with $\beta+\gamma<1$ contribute to the sum (3). Since the meson wave functions $\Phi_{M_\beta^2}^{b\bar{c}}(1-y)$ and

$\Phi^{ca}_{M^2}(z')$ in $F_{\beta\gamma}$ (cf. eq. 13) become fast oscillating functions for M^2_β , $M^2_\gamma \to \infty$ the leading asymptotic contributions arise from the boundaries of the y and z' integration. Let us discuss separately the two terms in eq. (13), which describe the direct coupling of the current and the coupling via bound state mesons, respectively. For $y=0$ the gluon pole at $y=0$, $z=0$ can be exploited, hence the $y=0$ boundary is favoured with respect to $y=1$. Thus, substituting $y \to y\frac{m^2}{s}$, $z \to z\frac{m^2}{s}$, $z' \to z'\frac{m^2}{s}$ or $1-z'\frac{m^2}{s}$ yields

$$F^{dir}_{\beta\gamma} \sim \frac{4ig\eta p_{\gamma-} e_c m^3}{s^2} \int_0^\infty dy\, dz\, dz' \frac{\frac{z\eta+y}{1+\eta}\Phi'_{M^2}(\frac{1}{1+\eta})}{(y+z\eta)^2} \times$$

$$\times (-1)^{\frac{\beta^2 s}{m^2\pi^2}} \Phi^c(y\beta^2)\{\Phi^c(z'\gamma^2) G^{c\bar{a}}(\frac{zm^2}{s}, \frac{1}{1+\eta'}; \frac{(p_\gamma - q)^2}{m^2}) +$$

$$+ (-1)^{\frac{\gamma^2 s}{m^2\pi^2}} \Phi^a(z'\gamma^2) G^{c\bar{a}}(\frac{zm^2}{s}, 1-\frac{zm^2}{s}\frac{\eta'}{1+\eta'}; \frac{(p_\gamma - q)^2}{m^2}),$$

(16)

where $\Phi'_{M^2}(x)$ denotes the derivative of $\Phi_{M^2}(x)$. To obtain eq. (16) we have used the scaling property (B5) of the wave function. Referring to the *Table* for the behaviour of η , $p_{\gamma-}$, $(p_\gamma - q)^2$ and using $G = O(\frac{1}{s})$ (cf. eqs. (B12, B13) we have

$$F^{dir}_{\beta\gamma} = O(\frac{1}{s^3}). \qquad (17)$$

The dominant contribution to the indirect coupling arises from $y=z=y'=z'=0$ because at this corner both gluon poles are exploited. With $y \to y\frac{m^2}{s}$.... we find

$$F^{ind}_{\beta\gamma} \sim \frac{4ig\eta R_\gamma - e_c m}{s} \int_0^\infty dy\,dz\,dy'dz' \frac{\frac{z\eta+y}{1+\eta}\,\Phi^{,b\bar{a}}(\frac{1}{M^2},\frac{1}{1+\eta})}{(1+z\eta)^2} \times$$

$$\times (-1)^{\frac{\beta^2 s}{m^2\pi^2}} \Phi^c(y\beta^2)\Phi^{\bar{c}}(z'\gamma^2) \frac{G^{c\bar{c}}(1-y'\frac{m^2}{s}; \frac{xs}{(x-1)m^2})}{(y'+z'\eta')^2} \times$$

$$\times [G^{c\bar{a}}(z\frac{m^2}{s}, \frac{1-y'\frac{m^2}{s}}{1+\eta'}; \frac{(p_\gamma - q)^2}{m^2}) -$$

$$- G^{c\bar{a}}(\frac{zm^2}{s}, \frac{1+\frac{z'\eta'm^2}{s}}{1+\eta'}; \frac{(p_\gamma - q)^2}{m^2})]. \qquad (18)$$

The behaviour of the Green functions is $O(\frac{1}{s})$ (comp. App. B) so we arrive at *

$$F^{ind}_{\beta\gamma} = O(\frac{1}{s^3}). \qquad (19)$$

Replacing the sum in (3) by integrals over the bound state masses we obtain the net behaviour

$$W^{(ii)}_{--} \sim \frac{1}{8\pi^6}\frac{s}{m^4} \int_{\beta+\gamma<1} d\beta^2 d\gamma^2 \frac{|F_{\beta\gamma}|^2}{\lambda^{1/2}(1,\beta^2,\gamma^2)} = O(\frac{1}{s^5}), \qquad (20)$$

which is again far too small to contribute to the partition function. If the cancellation between different ordered graphs of *fig. 4* represented by

---

* This estimate can further be improved by recognizing the additional cancellation between the G -functions in the bracket of eq. (18). This means that the indirect coupling is dominated by the direct one. The relation (19) is, however, sufficient for our purpose.

$$\Phi^{b\bar{a}}_{M^2}\left(\frac{1+z\eta-\frac{m^2}{s}}{1+\eta}\right)-\Phi^{b\bar{a}}_{M^2}\left(\frac{1-y\frac{m^2}{s}}{1+\eta}\right)-\frac{m^2}{s}\left(\frac{z\eta+y}{1+\eta}\right)\Phi'^{,b\bar{a}}_{M^2}\left(\frac{1}{1+\eta}\right)$$

is not taken into account, an individual ordered graph yields a contribution $O(\frac{1}{s^2})$ to $F_{\beta\gamma}$, which is also not enough to contribute in the Bjorken limit. It should be noted that this situation is rather different from the one encountered in the Regge limit [4,5]. We have thus found that the "Pomeron region" of the phase space does not contribute in the Bjorken limit even before the cancellation of diagrams is taken into account.

iii). a) M^2_β fix, $M^2_\gamma=\gamma^2 s$; b) M^2_γ fix, $M^2_\beta=\beta^2 s$

In the "+"-variant of the momenta (cf. the *Table*) the leading behaviour to $F^{dir}_{\beta\nu}$ comes from $z'=0,1$ due to the fast oscillating $\Phi^{c\bar{a}}_{M^2_\gamma}(z')$. Since the function $G^{c\bar{a}}$ vanishes (cf. eq. (B.10)) at $z'=1$. the contribution from $z'=0$ dominates. We get

$$F^{dir}_{\beta\gamma}(pq;p^{(+)}_\beta p^{(\div)}_\gamma)\sim\frac{1}{s}4ige_c p_- m\gamma^2(x+\gamma^2-x\gamma^2)(1-x)^2(1-\gamma^2)\times$$

$$\times\int_0^\infty dz'\int_0^1 dy\int_0^1 dz\,\frac{\Phi^{b\bar{a}}_{M^2}((1-x)(1-\gamma^2)+z(x+\gamma^2-x\gamma^2))-\Phi^{b\bar{a}}_{M^2}((1-y)(1-x)(1-\gamma^2))}{[(1-x)(1-\gamma^2)y+(x+\gamma^2-x\gamma^2)z]^2}$$

$$\times\Phi^{b\bar{c}}_{M^2_\beta}(1-y)\Phi^{c}(z'\gamma^2)G^{c\bar{a}}(z,\frac{x}{x+\gamma^2-x\gamma^2};(M^2/m^2-\frac{M^2_\beta/m^2}{(1-x)(1-\gamma^2)})(x+\gamma^2-x\gamma^2)). \qquad (21)$$

The leading contribution to $F^{ind}_{\beta\gamma}$ is due to $z'=0$, $y'=0$ and turns out to be

$$F^{ind}_{\underline{\beta}\gamma}(pq;p^{(+)}_{\beta}p^{(+)}_{\gamma}) = O(\frac{1}{s^2}) \qquad (22)$$

The same estimate (22) may also be derived for the "-" variant of the momenta. To complete the discussion we have to consider also the case b) M^2_{γ} fix , $M^2_{\beta} = \beta^2 s$. Because for both $\pm$ variants $(p_{\gamma} - q)^2 \to -\infty$, we get

$$F_{\underline{\beta}\gamma}(pq;p^{(\pm)}_{\beta}p^{(\pm)}_{\gamma}) = O(\frac{1}{s^2}). \qquad (23)$$

For $F_{\beta\underline{\gamma}}$ the role of M_{β} and M_{γ} as well as of (+) and (-) is, of course, changed. Hence, we arrive at the following contribution to W_{--}

$$W^{(iii)}_{--} \sim \frac{1}{8\pi^4 m^2}\Big(\sum_{M_{\beta}}\int_0^s dM^2_{\gamma}\frac{|F_{\underline{\beta}\gamma}(pq;p^{(+)}_{\beta}p^{(+)}_{\gamma})|^2}{\lambda^{1/2}(s,M^2_{\beta},M^2_{\gamma})} +$$

$$+\sum_{M_{\gamma}}\int_0^s dM^2_{\beta}\frac{|F_{\beta\underline{\gamma}}(pq;p^{(-)}_{\beta}p^{(-)}_{\gamma})|^2}{\lambda^{1/2}(s,M^2_{\beta},M^2_{\gamma})}\Big) \qquad (24)$$

and with eqs. (21), (B6) we obtain

$$\lim_{Bj} W(q^2,\nu) = f(x) \equiv (f^{b\bar{a}}(x) + f^{a\bar{b}}(x)), \qquad (25)$$

where

$$f^{b\bar{a}}(x) = \frac{e_c^2 m_c^2}{\pi N}(1-x)^2 \sum_{M_i^2}\int_0^1 d\rho\,(x+\rho-x\rho)^2(1-\rho)\times$$

$$\times\Big|\int_0^1 dy\int_0^1 dz\,\frac{\Phi^{b\bar{a}}_{M^2}(1-(1-z)(x+\rho-x\rho))-\Phi^{b\bar{a}}_{M^2}((1-y)(1-x)(1-\rho))}{[(1-x)(1-\rho)y+(x+\rho-x\rho)z]^2}\Phi^{c\bar{b}}_{M_i^2}(y)$$

$$\times G^{c\bar{a}}(z,\frac{x}{x+\rho-x\rho};(M^2/m^2-\frac{M_i^2/m^2}{(1-x)(1-\rho)})(x+\rho-x\rho))\Big|^2$$

and $f^{a\bar{b}}(x) = f^{\bar{b}a}(x)$ $(b \leftrightarrow a)$. (26)

The ρ-integration in (26) converges at $\rho = 0$ and 1. Moreover, the summation over M_i^2 converges since the expression under the sum is $O((\frac{1}{M_i^2})^2)$ for large M_i^2. These two convergence statements are necessary conditions for (26) to yield a finite coniribution in the Bjorken limit. In a similar way one may analyze the region $M_\beta^2 = O(\sqrt{s})$, $M_\gamma^2 = O(\sqrt{s^-})$, responsible for trajectory renormalization in the Regge limit[5]. By analogous considerations we find that the corresponding expression dies out as $q^2 \to -\infty$. Hence, the result (25) is the leading contribution of the cylinder graph in the Bjorken limit. We note that the expression (25) may dominate over the valence quarks of ref.[6] if the sea quarks are very heavy, $\frac{m_c^2}{N} >> m_a^2$, m_b^2.

To complete the discussion, we finally quote the behaviour of the structure function (25) in the limits $x \to 0$ and $x \to 1$, respectively. As in the case of the valence quarks, the behaviour of $f(x)$ at $x = 0$ turns out to be related to the Regge behaviour in just the way suggested by Abarbanel, Goldberger and Treiman[9]. With eq. (B9) we get, e.g.,

$$f^{b\bar{a}}(x) \underset{x\to 0}{=} x^{2\beta_c} \left| \frac{e_c^2 m_c^2}{\pi N} \sum_{M_i^2} \int_0^1 d\rho\, \rho^{2-2\beta_c} (1-\rho) \times \right.$$

$$\times \left| \int_0^1 dy \int_0^1 dz \, \frac{\Phi_{M^2}^{b\bar{a}}(1-\rho(1-z)) - \Phi_{M^2}^{b\bar{a}}((1-y)(1-\rho))}{[(1-\rho)\,y + \rho z]^2} \times \right.$$

$$\left. \left. \times \Phi_{M_i^2}^{c\bar{b}}(y)\, \hat{C}^{c\bar{a}}(z, (M^2/m^2 - \frac{M_i^2}{m^2(1-\rho)})\rho) \right|^2 \right| . \qquad (27)$$

Note that there is no x^{-1} behaviour being the signal of Pomeron exchange. Instead, the behaviour (27) is due

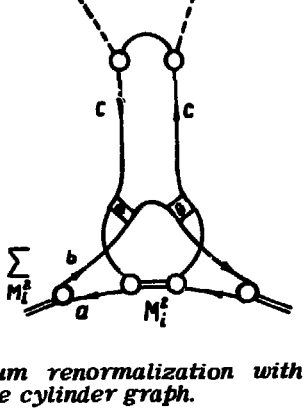

Fig. 6. Residuum renormalization with $(c\bar{c})$ *exchange obtained from the cylinder graph.*

to the exchange of an ordinary Regge trajectory ("f")with the intercept $\alpha_{c\bar{c}}(0)=-2\beta_c$ arising from the "residuum renormalization" graph shown in *fig. 6.* As β_c is a monotonously increasing function of m_c (cf. B3), we conclude that at $x=0$ the contribution of light sea quarks may dominate over the heavier valence quarks. Finally, we find from (26) using eqs. (A5, B12)

$$f^{b\bar{a}}(x) \underset{x\to 1}{\sim} A_c(1-x)^{2(\beta_a+\beta_b+\beta_c+1)} . \qquad (28)$$

Comparing eq. (28) with the valence quark behaviour [6] $\nu^2 W \underset{x\to 1}{\sim}(1-x)^{2\beta_{a,b}}$ we see that the contribution of the cylinder graph is suppressed for $x \to 1$ independent of the quark masses.

4. SUMMARY

We have investigated sea quark corrections of an order of $1/N$ to the structure function of deep inelastic scattering in QCD_2. The class of graphsconsidered con-

tains only one quark-antiquark loop and possesses the topology of the cylinder graph describing the dual bare Pomeron [7]. As our main result we find that there is no signal of a bare Pomeron in the quark partition function $f(x)$ as $x \to 0$ which is consistent with the conclusions of ref. [4,5] obtained for the Regge limit. However, to obtain this result the cancellation of different diagrams observed in the Regge limit is now unimportant. The cylinder graph yields also a finite contribution $f(x) \underset{x \to 0}{\sim} x^{-\alpha}$, α being the intercept of the exchanged "f" -trajectory, which may be interpreted as a residuum renormalization term. This expression may dominate at $x = 0$ over the valence quarks if the sea quarks are light.

It should be remarked that the absence of a bare Pomeron in QCD_2 is probably related to the lack of gluonic degrees of freedom and of gluonic bound states lying on the Pomeron trajectory.

ACKNOWLEDGEMENTS

We thank Dr. A.V.Efremov for useful discussions.

APPENDIX A

To be self-contained we list here some relevant formulas for QCD_2 needed in the text which have been discussed extensively in the literature [2,4]. The Feynman rules are *

gluon propagator: $P\frac{i}{k^2}$ (principal value)

dressed quark propagator: $$S_a(k) = \frac{i}{\not{k} - (m_a^2 - \frac{g^2 N}{\pi}) + i\epsilon} \quad \text{(A1)}$$

quark-gluon coupling: $-2ig$

---

* The gluon propagator used here differs by a factor of (-1) from that of ref. [4]. Therefore, we have also different signs in eqs. (A4) and (A6).

The normalized quark-antiquark meson vertex is defined by $(m^2 = \frac{g^2 N}{\pi})$

$$\Gamma_n^{a\bar{b}}(p,r) = -\frac{2igm}{r_-}\int_0^1 \frac{\Phi_n^{a\bar{b}}(y)}{(x-y)^2}dy; \quad x = \frac{p_-}{r_-} \qquad \text{(A2)}$$

or, if $x \in (0,1)$ and the bound state is on shell,

$$\Gamma_n(p,r) = -\frac{2ig}{mh(a,b)}\Phi_n^{a\bar{b}}(x), \qquad \text{(A3)}$$

where $\Phi_n^{a\bar{b}}(x)$ is the meson wave function of 't Hooft. The scattering matrix admits the decomposition $(x = \frac{p_-}{r_-}$, $x' = \frac{p'_-}{r_-})$

$$iT^{a\bar{b}}(p,p';r) = -\frac{4g^2 i}{r_-^2(x-x')^2} - \sum_n \frac{i}{r^2 - M_n^2}\Gamma_n^{a\bar{b}}(p,r)\Gamma_n^{a\bar{b}}(p',r). \qquad \text{(A4)}$$

It may be expressed by the Green function G,

$$G^{a\bar{b}}(x,y;\mu^2) = \sum_n \frac{\Phi_n^{a\bar{b}}(x)\Phi_n^{a\bar{b}}(y)}{\mu^2 - \mu_n^2} = G^{b\bar{a}}(1-x;1-y;\mu^2)$$
$$(\mu^2 = r^2/m^2) \qquad \text{(A5)}$$

in the following way

$$iT^{a\bar{b}}(p,p';r) = -\frac{4g^2 i}{r_-^2(x-x')^2} + \frac{4ig^2}{r_-^2}\int_0^1 dy \int_0^1 dz \frac{G^{a\bar{b}}(y,z;\frac{r^2}{m^2})}{(x-y)^2(x'-z)^2},$$

$$\text{if } x, x' \notin (0,1) \qquad \text{(A6a)}$$

$$iT^{a\bar{b}}(p,p';r) = \frac{4ig^2}{m^2 r_-}\frac{1}{h(a,b)}\int_0^1 dz \frac{G^{a\bar{b}}(x,z;\frac{r^2}{m^2})}{(x'-z)^2},$$

$$\text{if } x \in (0,1)$$
$$x' \notin (0,1) \qquad \text{(A6b)}$$

$$iT^{a\bar{b}}(p,p';r)=4ig^2\left(\frac{\delta(x-x')}{r_- m^2 h(a,b)}+\frac{G^{a\bar{b}}(x,x';\frac{r^2}{m^2})}{m^4 h(a,b)h(a',b')}\right),$$

if $x,x' \in (0,1)$. (A6c)

Finally, the quark form factor reads - $2ie_c Q^{c\bar{c}}(p,q)$,

$$Q^{c\bar{c}}(p,q)=1-\int_0^1 dy \int_0^1 dx' \frac{G^{c\bar{c}}(x',y;q^2/m^2)}{(x-x')^2}, \quad x=\frac{p_-}{-q_-} \qquad (A7)$$

or if $x \in (0,1)$

$$Q^{c\bar{c}}(p,q)=\frac{q_-}{m^2 h(c,c')}\int_0^1 G^{c\bar{c}}(x,y;\frac{q^2}{m^2})dy. \qquad (A8)$$

We have also considered a reduced G -function defined by

$$G^{a\bar{b}}(x;\mu^2)=\int_0^1 dy\, G^{a\bar{b}}(x,y;\mu^2). \qquad (A9)$$

APPENDIX B

We summarize here some properties of the functions $\Phi_n^{a\bar{b}}(x)$ and $G^{a\bar{b}}(x,y;\mu^2)$ (for details consult refs.[4, 6]).

$$\Phi_n^{a\bar{b}}(x)=(-1)^n \Phi_n^{b\bar{a}}(1-x), \qquad (B1)$$

$$\Phi_n^{a\bar{b}}(x) \underset{x\to 0}{\sim} x^{\beta_a} C^{a\bar{b}}, \qquad (B2)$$

where the power β_a is determined by

$$\frac{m_a^2}{m^2}+\pi\beta_a \cos\pi\beta_a = 1, \quad 0\le\beta_a<1. \qquad (B3)$$

Further

$$\Phi_n^{a\bar{b}}(x) \underset{n\to\infty}{\to} \sin\pi n x \qquad (B4)$$

$$\Phi_n^{a\bar{b}}\left(\frac{x}{\mu_n^2}\right) \underset{n\to\infty}{\to} \Phi^a(x); \qquad \mu_n^2 = \frac{M_n^2}{m^2} - \pi^2 n \,, \tag{B5}$$

$$\int_0^\infty dx\, \Phi^a(x) = \frac{\pi}{\sqrt{2}} \frac{m_a}{m} \,. \tag{B6}$$

The G-functions obey the following scaling relations

$$G^{a\bar{b}}\left(\frac{x}{-\mu^2}, \frac{y}{-\mu^2}; \mu^2\right) \xrightarrow[\mu^2\to-\infty]{} -\frac{1}{\pi^2}\int_0^\infty d\lambda \frac{\Phi^a(\lambda x)\Phi^a(\lambda y)}{1+\lambda}, \tag{B7}$$

$$G^{a\bar{b}}\left(\frac{x}{-\mu^2}; \mu^2\right) \xrightarrow[\mu^2\to-\infty]{} \frac{1}{\mu^2}\left(1 - \frac{\sqrt{2}\, m_a^2}{m\pi}\int_0^\infty d\lambda \frac{\Phi^a(\lambda)}{\lambda + x}\right). \tag{B8}$$

Finally, let us add some formulas not explicitly contained in the references cited. First, from (B2), (A5) we obtain

$$G^{a\bar{b}}(x, y; \mu^2) \underset{x\to 0}{\sim} x^{\beta_a} \hat{C}^{a\bar{b}}(y; \mu^2) \tag{B9}$$

$$G^{a\bar{b}}(1-x; y; \mu^2) = G^{b\bar{a}}(x, 1-y; \mu^2) \underset{x\to 0}{\sim} x^{\beta_b} \hat{C}^{b\bar{a}}(1-y; \mu^2). \tag{B10}$$

The completeness relation for the $\Phi_n^{a\bar{b}}$ yields

$$G^{a\bar{b}}(x, y; \mu^2) \underset{\mu^2\to-\infty}{\sim} \frac{1}{\mu^2}\delta(x-y) \tag{B11}$$

Using analogous techniques as those leading to eqs. (B7), (B8) we find the following additional estimates as $\mu^2 \to -\infty$ *

$$G^{a\bar{b}}\left(\frac{x}{-\mu^2}, y; \mu^2\right) = O\left(\left(\frac{1}{\mu^2}\right)^{1+\beta_a}\right), \tag{B12}$$

$$G^{a\bar{b}}\left(\frac{x}{-\mu^2}, 1-\frac{y}{-\mu^2}; \mu^2\right) = O\left(\left(\frac{1}{\mu^2}\right)^{1+\beta_a+\beta_b}\right) \,. \tag{B13}$$

---

* In ref. /4/ arguments are given in favour of $O\left(\left(\frac{1}{\mu^2}\right)^2\right)$ on the r.h.s. of (B13). We reproduce this falloff if we use the integral equation satisfied by G and (B11) under the integrals. As the approach to eq. (B11) is not uniform near $(x,y)=(0,1)$, the validity of such a behaviour is, however, not clear. Anyway, for our purposes the estimates (B12), (B13) are sufficient.

Table

	$\frac{M_\gamma^2}{s}\to 0,\ \frac{M_\beta^2}{s}\to 0$	$\frac{M_\gamma^2}{s}\to 0,\ M_\beta^2\sim\beta^2 s$	$M_\gamma^2\sim\gamma^2 s;\ \frac{M_\beta^2}{s}\to 0$	$M_\gamma^2\sim\gamma^2 s,\ M_\beta^2\sim\beta^2 s$
$p_{\beta-}$	$p_-(1-x)$ $\frac{M_\beta^2 p_-(1-x)}{s}$	$p_-(1-x)$ $\beta^2 p_-(1-x)$	$(1-\gamma^2)(1-x)p_-$ $\frac{M_\beta^2 p_-(1-x)}{s(1-\gamma^2)}$	$\frac{p_-(1-x)}{2}(1+\beta^2-\gamma^2\pm\lambda^{1/2}(1,\beta^2,\gamma^2))$
$p_{\gamma-}$	$\frac{M_\gamma^2 p_-(1-x)}{s}$ $p_-(1-x)$	$\frac{M_\gamma^2 p_-(1-x)}{s(1-\beta^2)}$ $(1-\beta^2)(1-x)p_-$	$\gamma^2 p_-(1-x)$ $p_-(1-x)$	$\frac{p_-(1-x)}{2}(1+\gamma^2-\beta^2\mp\lambda^{1/2}(1,\beta^2,\gamma^2))$
$(p-p_\beta)^2$	$(M^2-\frac{M_\beta^2}{1-x})x$ $-\frac{s}{1-x}$	$-\frac{x}{1-x}\beta^2 s$ $-\frac{s}{1-x}(1-\beta^2+\beta^2 x)$	$(M^2-\frac{M_\beta^2}{(1-\gamma^2)(1-x)})(x+\gamma^2-x\gamma^2)$ $-\frac{s(1-\gamma^2)}{1-x}$	$s\frac{\beta^2+\gamma^2-2\beta^2 x-1\pm\lambda^{1/2}(1,\beta^2,\gamma^2)}{2(1-x)}$
η	$\frac{x}{1-x}$ $\frac{s}{M_\beta^2(1-x)}$	$\frac{x}{1-x}$ $\frac{1}{\beta^2(1-x)}-1$	$\frac{1}{(1-\gamma^2)(1-x)}-1$ $\frac{s}{M_\beta^2}\frac{1-\gamma^2}{1-x}$	$\frac{2}{(1-x)(1+\beta^2-\gamma^2\pm\lambda^{1/2}(1,\beta^2,\gamma^2))}-1$
η'	$\frac{M_\gamma^2(1-x)}{xs}$ $\frac{1-x}{x}$	$\frac{M_\gamma^2(1-x)}{xs(1-\beta^2)}$ $\frac{(1-\beta^2)(1-x)}{x}$	$\gamma^2\frac{1-x}{x}$ $\frac{1-x}{x}$	$\frac{1-x}{2x}(1+\gamma^2-\beta^2\mp\lambda^{1/2}(1,\beta^2,\gamma^2))$

REFERENCES

1. *Gross D.J., Wilczek F. Phys. Rev., 1973, D8, p.3633; ibid., 1974, D9, p.980. Politzer H.D. Phys.Rep., 1974, 14, p.129.*
2. *"t Hooft G. Nucl.Phys., 1974, B72, p.461. Callan C.G. Jr., Coote N., Gross D.J. Phys.Rev., 1976, D13, p.1649. Marinov M.S., Perelomov A.M., Terent'ev M.V. JETP. Lett., 1974, 20, p.225.*
3. *Ebert D., Pervushin V.N. JINR, E2-10730, Dubna, 1977; ibid., E2-10731, Dubna, 1977.*
4. *Brower R.C. et al. Phys.Lett., 1976, 65B, p.249 and CERN Preprints TH 2283, 2295, 1977; Ellis J. Applications of QCD (Zakopane Lectures), 1977.*
5. *Einhorn M.B., Nussinov S., Rabinovici E. Michigan prepr., UM HE, 1976, 76-39. Einhorn M.B., Rabinovici E. Nucl.Phys., 1977, B128, p.421.*
6. *Einhorn M.B. Phys.Rev., 1976, D14, p.3451.*
7. *"Dual Theory" - ed. by M.Jacob (North-Holland, Amsterdam, 1974); Ebert D., Otto H.J. A Survey on Dual Tree and Loop Amplitudes. Fortschr. d. Phys., 1977, 25, p.203.*
8. *Kripfganz J., Schmidt M.G. Nucl.Phys., 1977, B125, p.323.*
9. *Abarbanel H.D.J., Goldberger M.L., Treiman S.B. Phys.Rev.Lett., 1969, 22, p.500.*

Received by Publishing Department on December 30, 1977.

SUBJECT CATEGORIES

OF THE JINR PUBLICATIONS

Index	Subject
1.	High energy experimental physics
2.	High energy theoretical physics
3.	Low energy experimental physics
4.	Low energy theoretical physics
5.	Mathematics
6.	Nuclear spectroscopy and radiochemistry
7.	Heavy ion physics
8.	Cryogenics
9.	Accelerators
10.	Automatization of data processing
11.	Computing mathematics and technique
12.	Chemistry
13.	Experimental techniques and methods
14.	Solid state physics. Liquids
15.	Experimental physics of nuclear reactions at low energies
16.	Health physics. Shieldings
17.	Theory of condensed matter

Издательский отдел Объединенного института ядерных исследований.
Заказ 24336. Тираж 650. Уч.-изд. листов 1,51.
Редактор Э.В. Ивашкевич. Подписано к печати 30.01.78 г.
Корректор Р.Д. Фомина.

СООБЩЕНИЯ
ОБЪЕДИНЕННОГО
ИНСТИТУТА
ЯДЕРНЫХ
ИССЛЕДОВАНИЙ
ДУБНА

E2 - 11222

H.Dorn, D.Ebert, V.N.Pervushin

QUARK SEA CONTRIBUTIONS TO DEEP INELASTIC SCATTERING IN TWO-DIMENSIONAL QCD

1978

E2 - 11222

H.Dorn, D.Ebert, V.N.Pervushin

QUARK SEA CONTRIBUTIONS TO DEEP INELASTIC SCATTERING IN TWO-DIMENSIONAL QCD

Дорн Х., Эберт Д., Первушин В.Н. Е2 - 11222

Вклад кварков из моря (sea–quarks) в глубоконеупругое рассеяние в двумерной К.Х.Д.

В рамках двумерной квантовой хромодинамики в бъеркеновском пределе найден вклад невалентных кварков (sea–quarks) в структурную функцию глубоконеупругого рассеяния. При больших N рассматриваются "цилиндрические" диаграммы, вклад которых интерпретируется как перенормировка вычета f -траектории с квантовыми числами вакуума.

Работа выполнена в Лаборатории теоретической физики ОИЯИ.

Сообщение Объединенного института ядерных исследований. Дубна 1978

Dorn H., Ebert D., Pervushin V.N. E2 - 11222

Quark Sea Contributions to Deep Inelastic Scattering in Two-Dimensional QCD

Quark sea contributions to the partition function are studied in the Bjorken limit using two-dimensional QCD in the 1/N approximation. The cylinder graphs considered yield a contribution which is associated to "residuum renormalization" of the "f" - trajectory exchanged in the vacuum channel.

The investigation has been performed at the Laboratory of Theoretical Physics, JINR.

Communication of the Joint Institute for Nuclear Research. Dubna 1978

1. INTRODUCTION

QCD, the non-Abelian gauge theory of coloured quarks and gluons, is at present the most prominent candidate for a theory describing the hadronic world. This rests mainly on the property of asymptotic freedom and the possibility that the infrared instability of QCD confines the quarks [1]. Despite many attempts quark confinement has, however, not yet been proved for four-dimensional QCD. In this situation it is of importance that two-dimensional QCD (QCD_2) can be solved in leading order of an $1/N$ expansion, where N is the number of colours, yielding an infinite number of bound state mesons as well as confinement of quarks and gluons [2]. A transparent formulation of QCD_2 in terms of bound state fields may further be obtained by using functional methods [3]. Moreover, there exists an extensive literature [4,5] on the Regge asymptotic behaviour of scattering amplitudes for this model. Although confinement is almost trivial in two dimensions, a merit of QCD_2 is to provide us with an example of how final bound state hadrons in deep inelastic scattering realize Bjorken scaling in a way demanded by the asymptotic freedom of the theory. Einhorn [6] has evaluated the Bjorken limit of the graphs shown in *fig. 1* which yield the leading order contribution to deep inelastic scattering by the valence quarks inside the mesons. The quark partition function is in this case determined by the square of the meson bound state wave function. There is, however, an additional possibility for a virtual photon to scatter with quark-antiquark pairs $c\bar{c}$ created by gluons out of the quark sea. It is of importance to study such effects in order to understand the consequences of the sea and to check whether the dynamical picture of hadrons is self-consistent.

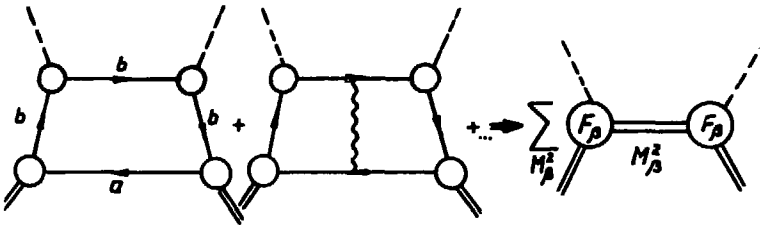

Fig. 1. Inelastic scattering by valence quarks as the square of form factors[6].

In this paper we shall investigate a contribution of sea quarks to the structure function of deep inelastic scattering in QCD_2. For simplicity, we shall consider the correction terms of an order of $1/N$ containing only one $c\bar{c}$ -loop which are depicted in *fig. 2a*. This class of diagrams is particularly interesting because the graphs possess the topology of the bare Pomeron of the dual model [7] (cf. *fig. 2b*). The paper is organized as follows. In Sec. 2 we derive the formula of the quark sea contributions to the virtual Compton amplitude. Section 3 is devoted to the study of the Bjorken limit including a detailed investigation of different regions of the phase space. Section 4 contains a summary of the results. There are two appendices presenting some formulas and results that are needed in the text.

2. *DEEP INELASTIC SCATTERING*

We shall consider quantum chromodynamics in two-dimensions (QCD_2) which was investigated in the limit $N \to \infty$, g^2N fix, in leading order of $1/N$ in the light-cone gauge[2], where g is the gauge coupling constant and N the number of colours (for the Feynman rules,

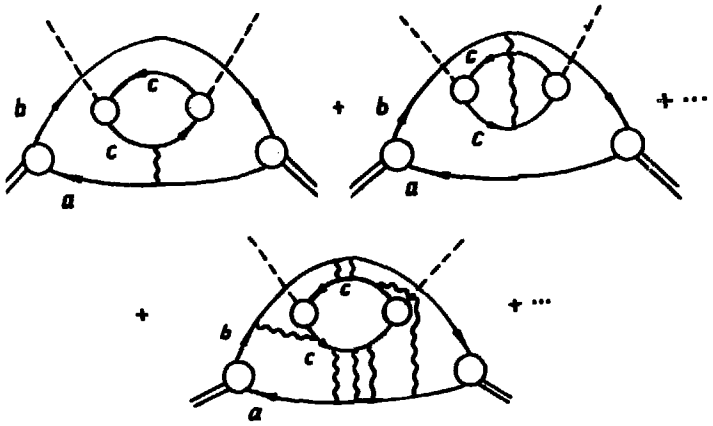

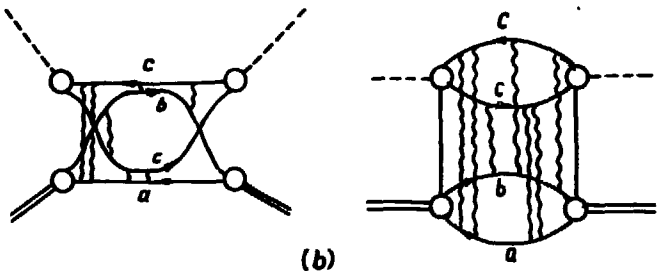

Fig. 2. a) Inelastic scattering by a pair $c\bar{c}$ *of sea quarks. b) Equivalent representation of a process with sea quarks as a twisted loop or cylinder graph with gluonic exchange, respectively.*

see app. A). The two-dimensional analogue of the deep inelastic scattering $eM \to eX$ of an electron by a bound state meson M of momentum p is described by the Bjorken limit of the tensor $W_{\mu\nu} = \int d^2x e^{iqx} \langle M,p|j_\mu(x)j_\nu(0)|M,p\rangle$, which is the discontinuity of the corresponding virtual Compton amplitude in the variable $s=(p+q)^2$. $W_{\mu\nu}$ may be expressed by the structure function $W(q^2,\nu)$ *

$$W_{\mu\nu} = (p_\mu - \frac{q_\mu \nu}{q^2})(p_\nu - \frac{q_\nu \nu}{q^2}) W(q^2, \nu), \qquad (1)$$

where, as usual, we define

$$\nu = p \cdot q, \quad x_{Bj} = \frac{-q^2}{2\nu}; \quad p^2 = M^2.$$

The scattering of a virtual photon with the valence quarks b and $\bar{a}$ forming the bound state meson M (cf. *fig. 1*) has been studied in leading order of the 1/N expansion by Einhorn /6/. Its contribution is just given by the square of the meson form factor summed over all intermediate meson resonances. A virtual photon may, however, also scatter with a quark-antiquark pair $c\bar{c}$ created by gluons out of the quark sea. In the following we shall investigate the contribution of such sea quarks to $W_{\mu\nu}$ restricting ourselves, for simplicity, to the graphs of *fig. 2a* containing only one $c\bar{c}$-loop. We may redraw these graphs in the form of a twisted loop or cylinder graph with two quark boundaries and no handles (cf. *fig. 2b*). Thus, it becomes evident that the set of graphs considered possesses just the topology of the bare Pomeron of the dual model /7/. Calculating the discontinuity of the above graphs quark singularities should cancel as usual, because of confinement, so that intermediate bound state mesons contribute alone. Hence, we have to consider only the discontinuity of the graph shown in *fig. 3a* and to sum over the intermediate mesons. Let us denote the ampli-

---

* In QCD_2 there exists only one independent structure function owing to the relation ($q^2 < 0$)

$$p_\mu = \frac{\nu}{q^2} q_\mu + \frac{\sqrt{\nu^2 - q^2 M^2}}{q^2} \epsilon_{\mu\sigma} q^\sigma \operatorname{sgn} q_1 .$$

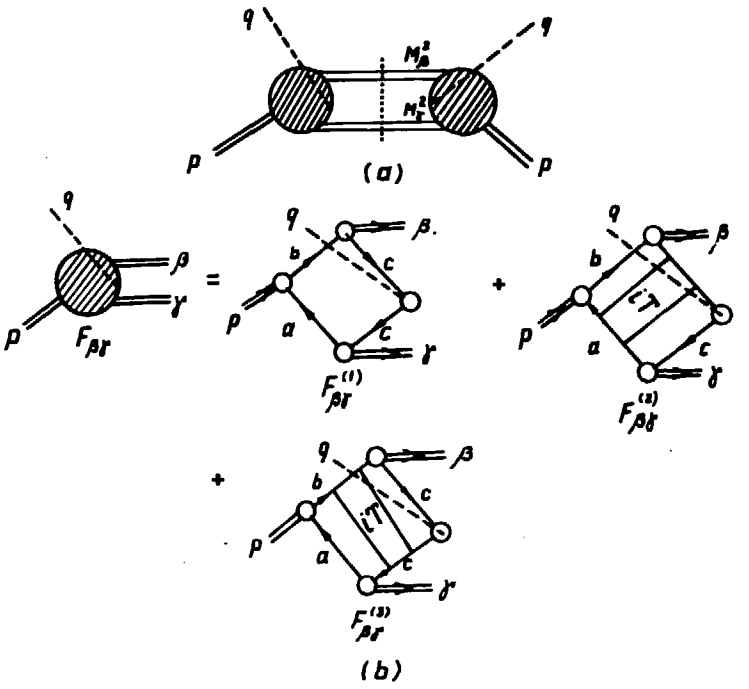

Fig. 3. a) The absorptive part of the virtual Compton amplitude with two intermediate mesonic states. b) The amplitude $F_{\beta\gamma}$ *to leading order in* $1/N$.

tude drawn in *fig. 3b* by $F_{\beta\gamma}(pq;p_\beta p_\gamma)$. T is the quark-antiquark scattering amplitude. It is simplest to calculate W_{--} which is given by

$$W_{--} = \sum_{\beta,\gamma} \int \frac{d^2k}{(2\pi)^2} |F_{\beta\gamma}(pq;p+q-k,k)|^2 \delta_+(k^2-M_\gamma^2) \times$$

$$\times \delta_+((p+q-k)^2-M_\beta^2). \qquad (2)$$

Performing the integration, we get

$$W_{--} = \frac{1}{8\pi^2} \sum_{\beta,\gamma} \int_{(M_\beta+M_\gamma)^2<(p+q)^2} \lambda^{-1/2}(s, M_\beta^2, M_\gamma^2) \sum_{i=\pm} |F_{\beta\gamma}(pq; p_\beta^{(i)} p_\gamma^{(i)})|^2, \tag{3}$$

where λ is the usual triangular function and

$$p_{\gamma-}^{(\pm)} = \frac{s+M_\gamma^2-M_\beta^2 \mp \lambda^{1/2}(s, M_\beta^2, M_\gamma^2)}{4(p_+ + q_+)},$$

$$p_{\beta-}^{(\pm)} = \frac{s+M_\beta^2-M_\gamma^2 \pm \lambda^{1/2}(s, M_\beta^2, M_\gamma^2)}{4(p_+ + q_+)}, \tag{4}$$

$$p_\pm = \frac{1}{\sqrt{2}}(p_0 \pm p_1); \quad s = (p+q)^2, \quad p_\beta^2 = M_\beta^2, \text{etc.}$$

The two upper signs $\pm$ of the momenta (4) correspond to whether the mesons β, γ are right-moving or left-moving.

2.1. Kinematics in Einhorn's Reference Frame

We consider a system, where $q_- < 0$, q_- fix (q ingoing). Defining $x = -\frac{q_-}{p_-}$ we find the following relations in the Bjorken limit $\nu(s) \to \infty$, $q^2 \to -\infty$, x_{Bj} fixed,

$$x_{Bj} = x + O(\frac{1}{s}),$$

$$q^2 = -s\frac{x}{1-x} + O(1); \quad \nu = \frac{s}{2(1-x)} + O(1), \tag{5}$$

$$p_- + q_- = p_-(1-x); \quad p_+ + q_+ = \frac{s}{2p_-(1-x)}.$$

For further reference, we list also some ordering relations between different "-" components of momenta involved. Since p , p_γ , p_β are the momenta of ingoing or outgoing particles, we have

$$p_- , p_{\gamma -} , p_{\beta -} > 0 .$$

Together with $q_- < 0$ and momentum conservation, this yields

$$p_- - p_{\beta -} = p_{\gamma -} - q_- > 0 , \quad p_- - p_{\gamma -} = p_{\beta -} - q_- > 0 . \tag{6}$$

2.2. *The Amplitude* $F_{\beta\gamma}$

The diagrams of *fig. 3b* can now be calculated using the expressions for the quark propagator, the T -matrix, the vertex function and the quark formfactor of ref. [6] (see also appendix A). Let us consider, for example, the diagram $F^{(2)}_{\beta\gamma}$. We get

$$F^{(2)}_{\beta\gamma} = -2ie_c N^2 \int \frac{d^2k}{(2\pi)^2} \int \frac{d^2\ell}{(2\pi)^2} S_c(k-q) Q^{c\bar{c}}(k,q) S_c(k) \times$$

$$\times \Gamma^{c\bar{a}}(k, p_\gamma) S_a(k - p_\gamma) \cdot iT(k - p_\gamma, \ell - p; (q - p_\gamma)^2) S_a(\ell - p) \times$$

$$\times \Gamma^{b\bar{a}}(\ell, p) S_b(\ell) \Gamma^{b\bar{c}}(\ell, p_\beta) S_c(\ell - p_\beta) . \tag{7}$$

As only the quark propagators depend on the "+" components of the momenta, the respective loop integration over k_+ , ℓ_+ can easily be done. In the case of three quark propagators we obtain, e.g.,

$$\int dk_+ S_i(k_i) S_j(k_j) S_\ell(k_\ell) =$$

$$= \pi \{ \Theta(-k_{i-}) \Theta(k_{j-}) \Theta(k_{\ell-}) - \Theta(k_{i-}) \Theta(-k_{j-}) \Theta(-k_{\ell-}) \} h(i,j) h(i,\ell)$$

$$+ \{ \Theta(k_{i-}) \Theta(-k_{j-}) \Theta(k_{\ell-}) - \Theta(-k_{i-}) \Theta(k_{j-}) \Theta(-k_{\ell-}) \} h(j,i) h(j,\ell)$$

$$+\{\Theta(k_{i_-})\Theta(k_{j_-})\Theta(-k_{\ell_-}) - \Theta(-k_{i_-})\Theta(-k_{j_-})\Theta(k_{\ell_-})\}\,h(\ell,i)h(\ell,j)], \tag{8}$$

where

$$h(i,j) = \frac{(k_i - k_j)_-}{\frac{m_i^2 - m^2}{k_{i_-}/(k_i - k_j)_-} - \frac{m_j^2 - m^2}{k_{j_-}/(k_i - k_j)_-} - (k_i - k_j)^2} = -h(j,i),$$

$$m^2 = \frac{g^2 N}{\pi}. \tag{9}$$

A similar formula holds in the case of four internal propagators. The single terms in the r.h.s. of eq. (8) can be visualized graphically by x_- – "time" ordered graphs [4,6] where quark lines are directed to the right (left) if their momentum k_- is positive (negative). This rule may be extended to the momenta of the bound states and the current, too. In most of such ordered graphs the above factors h may be absorbed by the vertex function, the quark form factor or the T-matrix, respectively, [4] (see eqs. (A3, A6, A8) of App. A). Applying eq.(8) to eq. (7) and using eqs. (A.3), (A.6) in a way to cancel as many h's as possible, we arrive at the graphs of *fig.4d-i*. These graphs are to be understood with the following modified rules:

gluon line: $\frac{1}{k_-^2}$

quark line: 1 (10)

gluon-quark vertex: 1

meson wave functions: $\Phi_n^{a\bar{b}}(k_-/p_{n-})$.

Note that there appear gluon propagators in the diagrams because we have used eq. (A.2) in order to "turn" around a quark with $x = \frac{k_-}{p_-} < 0$ at a vertex into a quark with

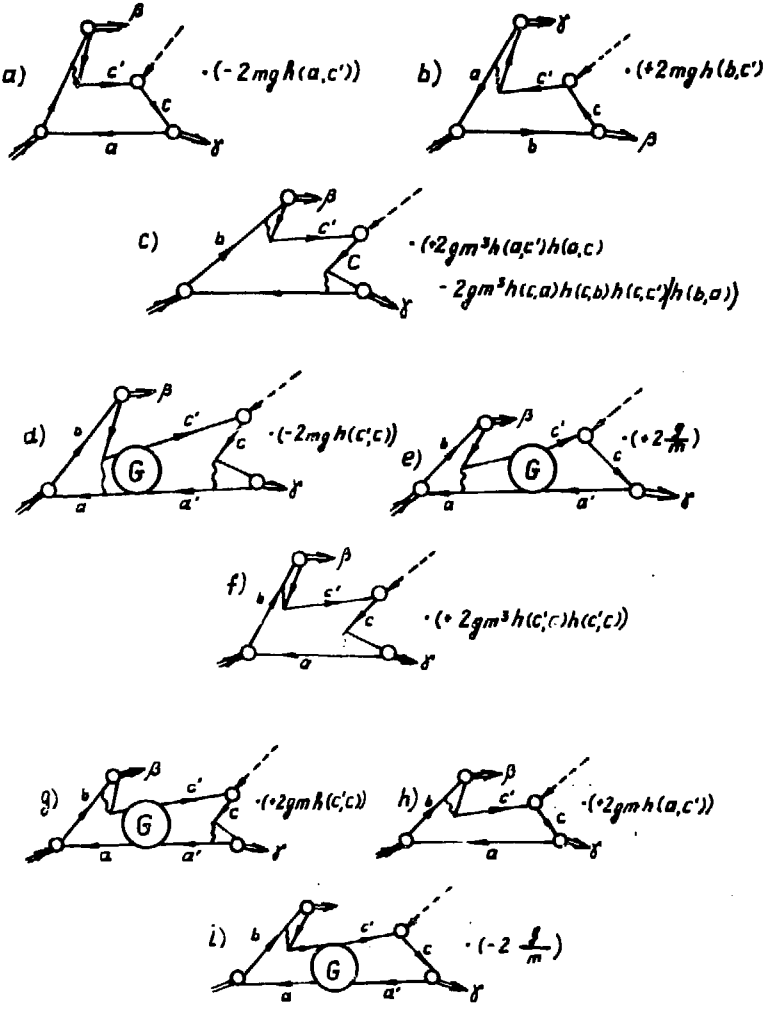

Fig. 4. a)-i). "Time" ordered perturbation theoretical diagrams contributing to $F_{\beta\gamma}^{(1)}$ *(a-c) and to* $F_{\beta\gamma}^{(2)}$ *(d-i). (Momenta* k_c, k_c' *of c-quarks are denoted by* c, c' *etc.).*

$0 \leq x \leq 1$. The quark form factor is yet unchanged. All remaining factors are written down explicitly as a number multiplying the expression of the corresponding graph obtained by means of (10). The ordered graphs belonging to the contributions $F^{(1)}_{\beta\gamma}$, $F^{(3)}_{\beta\gamma}$ of *fig. 3* may be derived analogously. The graphs of $F^{(1)}_{\beta\gamma}$ are depicted in *fig. 4a-c*. Finally, the graphs belonging to $F^{(3)}_{\beta\gamma}$ may be obtained from those of $F^{(2)}_{\beta\gamma}$ by replacing $\beta \to \gamma$ and reversing the direction of the quark lines. Now *4a)* cancels *4h)*, and *4b)* cancels the analogous graph of $F^{(3)}_{\beta\gamma}$. The remaining 11 ordered graphs can be collected into three groups if we use the concepts of the three-meson vertex /2,4/, the meson form factor /6/ and an irreducible four-point coupling between a current and three mesons. The graphs *4d), e), g), i)* and their analogs of $F^{(3)}_{\beta\gamma}$ are represented by the second and third diagrams of *fig. 5*, respectively. The remaining graphs *4c), f)* and an analogous graph from $F^{(3)}_{\beta\gamma}$ constitute the irreducible four-point coupling which by the algebraic identity

$$\left(h(a,c')h(a,c) - \frac{h(c,a)h(c,b)h(c,c')}{h(b,a)}\right) + h(c',a)h(c',c) + h(c',b)h(c',c) = 0. \tag{11}$$

is identically zero. In the next step we use eq. (A.8) to

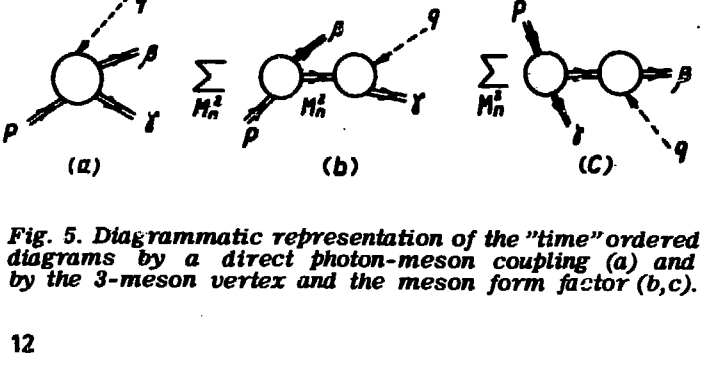

Fig. 5. Diagrammatic representation of the "time" ordered diagrams by a direct photon-meson coupling (a) and by the 3-meson vertex and the meson form factor (b,c).

eliminate the last h -factors. After some substitutions in the integrals involved we, finally, arrive at

$$F_{\beta\gamma}(p,q;p_\beta p_\gamma)=F_{\underline{\beta}\gamma}(\dots)+F_{\beta\underline{\gamma}}(\dots) \tag{12}$$

$$F_{\underline{\beta}\gamma}(p,q;p_\beta p_\gamma)=\frac{4ig\eta p_{\gamma-}c_c}{m}\int_0^1 dydzdy'dz'\times$$

$$\times\frac{\Phi_{M^2}^{b\bar{a}}\left(\frac{1+z\eta}{1+\eta}\right)-\Phi_{M^2}^{b\bar{a}}\left(\frac{1-y}{1+\eta}\right)}{(y+z\eta)^2}\times\Phi_{M_\beta^2}^{b\bar{c}}(1-y)\Phi_{M_\gamma^2}^{c\bar{a}}(z')\times$$

$$\times\{G^{c\bar{a}}\left(z,\frac{1+z'\eta'}{1+\eta'};\frac{(p_\gamma-q)^2}{m^2}\right)-$$

$$-\frac{G^{c\bar{c}}\left(1-y';\frac{q^2}{m^2}\right)}{(y'+z'\eta')^2}\left[G^{c\bar{a}}\left(z,\frac{1+z'\eta'}{1+\eta'};\frac{(p_\gamma-q)^2}{m^2}\right)-G^{c\bar{a}}\left(z,\frac{1-y'}{1+\eta'};\frac{(p_\gamma-q)^2}{m^2}\right)\right]\}, \tag{13}$$

$$\eta=\frac{(p-p_\beta)_-}{p_{\beta-}},\quad \eta'=-\frac{p_{\gamma-}}{q_-},$$

where the Green functions $G(x,y;p^2)$, $G(x;p^2)$ are defined in the appendix, and we have written $\Phi_{M_n^2}$ instead of Φ_n ($M_n^2\sim\pi^2m^2n$). The above expression $F_{\beta\gamma}$ represents the graphs *4d), e), g), i)* = second graph of *fig. 5*. $F_{\beta\underline{\gamma}}$ corresponds to the third graph of *fig. 5* and may be obtained from (13) by the change $\beta\leftrightarrow\gamma$ and a suitable change of the flavour indices. We mention that the above ordered graph scheme depends on the reference frame and the kinematical region under consideration.

3. *ASYMPTOTIC BEHAVIOUR OF* $F_{\beta\gamma}$ *IN THE BJORKEN LIMIT*

In the following we shall compute the contribution of the above graphs to the partition function $f(x)$ for deep inelastic scattering by sea quarks *

$$f(x) = \lim_{Bj} \nu^2 W(q^2, \nu). \tag{14}$$

Before estimating different contributions of the phase space to the sum in eq. (3), let us recall briefly the results obtained for the *Regge limit* of the cylinder graph with external mesons only [4,5]. As has been found, the phase space region M_β^2 , $M_\gamma^2 = O(1)$ yields a Regge-Regge cut contribution. From the region $M_\beta^2 = O(s)$, $M_\gamma^2 = O(s)$ each of the ordered diagrams gets an asymptotic contribution reminiscent of Pomeron exchange. There works, however, in the Regge limit an intriguing cancellation between different asymptotic contributions so that really no net bare Pomeron in QCD_2 does appear. Finally, the regions $M_\beta^2 = O(s)$, M_γ^2 fix (M_β^2 fix, $M_\gamma^2 = O(s)$) and $M_\beta^2, M_\gamma^2 = O(\sqrt{s})$ lead to a residuum or trajectory renormalization of the ordinary "f"-trajectory, respectively, that breaks exchange degeneracy.

Let us now evaluate the contribution of the analogous phase space regions to deep inelastic scattering and ask whether a cancellation mechanism works also in the Bjorken limit of the cylinder graph with external currents. This question is not trivially answered because the cancellation may be incomplete for processes with external currents [8]. Moreover, there contribute other sets of or-

---

* Using dimensional counting arguments one should take into consideration that in QCD_2 coupling constants have a mass dimension $[g;e] = 1$. With $[\langle M, p \rangle] = 1$, $[j_\mu]$ (including e_c) $= 2$ we find $[W_{\_\_}] = 2$ and $[W] = 0$. The partition function contains then a dimensional factor (comp. eq. 26).

dered diagrams in the Bjorken region ($q_- < 0$) than in the Regge region ($q_- > 0$).

i). $M_\beta^2, M_\gamma^2 = O(1)$

We start with the discussion of $F_{\beta\gamma}$. The relevant kinematics following from eqs. (4), (5) has been grouped together in the *Table*. Using eqs. (B9,B12) we find

$$F_{\beta\gamma}(pq;p_\beta^{(+)}p_\gamma^{(+)}) = \frac{4igxp_-e_c}{m}\left(\frac{M_\gamma^2}{s}\right)^{1+\beta_a} \times$$

$$\times\left(\frac{1-x}{x}\right)^{\beta_a}\int_0^1 dydzdz' \frac{\Phi_{M^2}^{b\bar{a}}(1-x+zx) - \Phi_{M^2}^{b\bar{a}}((1-y)(1-x))}{\left(y+z\frac{x}{1-x}\right)^2} \times$$

$$\times\Phi_{M_\beta^2}^{b\bar{c}}(1-y)\Phi_{M_\gamma^2}^{c\bar{a}}(z')(1-z')^{\beta_a}\hat{C}^{a\bar{c}}\left(z, M^2x - M_\beta^2\frac{x}{1-x}\right) + O\left(\frac{1}{s^{1+\beta_a}}\right) =$$

$$= O\left(\frac{1}{s}\right). \qquad (15)$$

For illustration, we have written down in eq. (15) the contribution from the direct coupling of the current. In a similar manner one proves $F_{\beta\gamma}(pq;p_\beta^{(-)}p_\gamma^{(-)}) = O\left(\frac{1}{s}\right)$. Further, taking into account $\lambda^{-1/2}(s, M_\beta^2, M_\gamma^2) \sim 1/s$, we get $W^{(i)}(q^2,\nu) = O(1/s^3)$. Thus, there is no contribution to the partition function $f(x)$.

ii). $M_\beta^2 = \beta^2 s, M_\gamma^2 = \gamma^2 s$

Now for fixed β, γ masses with $\beta+\gamma<1$ contribute to the sum (3). Since the meson wave functions $\Phi_{M_\beta^2}^{b\bar{c}}(1-y)$ and

$\Phi^{ca}_{M^2}(z')$ in $F_{\beta\gamma}$ (cf. eq. 13) become fast oscillating functions for M^2_β , $M^2_\gamma \to \infty$ the leading asymptotic contributions arise from the boundaries of the y and z' integration. Let us discuss separately the two terms in eq. (13), which describe the direct coupling of the current and the coupling via bound state mesons, respectively. For $y=0$ the gluon pole at $y=0$, $z=0$ can be exploited, hence the $y=0$ boundary is favoured with respect to $y=1$. Thus, substituting $y \to y\frac{m^2}{s}$, $z \to z\frac{m^2}{s}$, $z' \to z'\frac{m^2}{s}$ or $1-z'\frac{m^2}{s}$ yields

$$F^{dir}_{\beta\gamma} \sim \frac{4ig\eta p_{\gamma-} e_c m^3}{s^2} \int_0^\infty dy\, dz\, dz' \frac{\frac{z\eta+y}{1+\eta}\Phi'_{M^2}(\frac{1}{1+\eta})}{(y+z\eta)^2} \times$$

$$\times (-1)^{\frac{\beta^2 s}{m^2\pi^2}} \Phi^c(y\beta^2)\{\Phi^c(z'\gamma^2) G^{c\bar{a}}(\frac{zm^2}{s}, \frac{1}{1+\eta'}; \frac{(p_\gamma - q)^2}{m^2}) +$$

$$+ (-1)^{\frac{\gamma^2 s}{m^2\pi^2}} \Phi^a(z'\gamma^2) G^{c\bar{a}}(\frac{zm^2}{s}, 1-\frac{zm^2}{s}\frac{\eta'}{1+\eta'}; \frac{(p_\gamma - q)^2}{m^2}),$$

(16)

where $\Phi'_{M^2}(x)$ denotes the derivative of $\Phi_{M^2}(x)$. To obtain eq. (16) we have used the scaling property (B5) of the wave function. Referring to the *Table* for the behaviour of η , $p_{\gamma-}$, $(p_\gamma - q)^2$ and using $G = O(\frac{1}{s})$ (cf. eqs. (B12, B13) we have

$$F^{dir}_{\beta\gamma} = O(\frac{1}{s^3}). \qquad (17)$$

The dominant contribution to the indirect coupling arises from $y=z=y'=z'=0$ because at this corner both gluon poles are exploited. With $y \to y\frac{m^2}{s}$.... we find

$$F^{ind}_{\beta\gamma} \sim \frac{4ig\eta R_\gamma - e_c m}{s} \int_0^\infty dy\,dz\,dy'dz' \frac{\frac{z\eta+y}{1+\eta}\,\Phi^{,b\bar{a}}(\frac{1}{M^2},\frac{1}{1+\eta})}{(1+z\eta)^2} \times$$

$$\times (-1)^{\frac{\beta^2 s}{m^2\pi^2}} \Phi^c(y\beta^2)\Phi^{\bar{c}}(z'\gamma^2) \frac{G^{c\bar{c}}(1-y'\frac{m^2}{s}; \frac{xs}{(x-1)m^2})}{(y'+z'\eta')^2} \times$$

$$\times [G^{c\bar{a}}(z\frac{m^2}{s}, \frac{1-y'\frac{m^2}{s}}{1+\eta'}; \frac{(p_\gamma - q)^2}{m^2}) -$$

$$- G^{c\bar{a}}(\frac{zm^2}{s}, \frac{1+\frac{z'\eta'm^2}{s}}{1+\eta'}; \frac{(p_\gamma - q)^2}{m^2})]. \qquad (18)$$

The behaviour of the Green functions is $O(\frac{1}{s})$ (comp. App. B) so we arrive at *

$$F^{ind}_{\beta\gamma} = O(\frac{1}{s^3}). \qquad (19)$$

Replacing the sum in (3) by integrals over the bound state masses we obtain the net behaviour

$$W^{(ii)}_{--} \sim \frac{1}{8\pi^6}\frac{s}{m^4} \int_{\beta+\gamma<1} d\beta^2 d\gamma^2 \frac{|F_{\beta\gamma}|^2}{\lambda^{1/2}(1,\beta^2,\gamma^2)} = O(\frac{1}{s^5}), \qquad (20)$$

which is again far too small to contribute to the partition function. If the cancellation between different ordered graphs of *fig. 4* represented by

---

* This estimate can further be improved by recognizing the additional cancellation between the G -functions in the bracket of eq. (18). This means that the indirect coupling is dominated by the direct one. The relation (19) is, however, sufficient for our purpose.

$$\Phi^{b\bar{a}}_{M^2}\left(\frac{1+z\eta-\frac{m^2}{s}}{1+\eta}\right)-\Phi^{b\bar{a}}_{M^2}\left(\frac{1-y\frac{m^2}{s}}{1+\eta}\right)-\frac{m^2}{s}\left(\frac{z\eta+y}{1+\eta}\right)\Phi'^{,b\bar{a}}_{M^2}\left(\frac{1}{1+\eta}\right)$$

is not taken into account, an individual ordered graph yields a contribution $O(\frac{1}{s^2})$ to $F_{\beta\gamma}$, which is also not enough to contribute in the Bjorken limit. It should be noted that this situation is rather different from the one encountered in the Regge limit [4,5]. We have thus found that the "Pomeron region" of the phase space does not contribute in the Bjorken limit even before the cancellation of diagrams is taken into account.

iii). a) M^2_β fix, $M^2_\gamma=\gamma^2 s$; b) M^2_γ fix, $M^2_\beta=\beta^2 s$

In the "+"-variant of the momenta (cf. the *Table*) the leading behaviour to $F^{dir}_{\beta\nu}$ comes from $z'=0,1$ due to the fast oscillating $\Phi^{c\bar{a}}_{M^2_\gamma}(z')$. Since the function $G^{c\bar{a}}$ vanishes (cf. eq. (B.10)) at $z'=1$. the contribution from $z'=0$ dominates. We get

$$F^{dir}_{\beta\gamma}(pq;p^{(+)}_\beta p^{(\div)}_\gamma)\sim\frac{1}{s}4ige_c p_- m\gamma^2(x+\gamma^2-x\gamma^2)(1-x)^2(1-\gamma^2)\times$$

$$\times\int_0^\infty dz'\int_0^1 dy\int_0^1 dz\,\frac{\Phi^{b\bar{a}}_{M^2}((1-x)(1-\gamma^2)+z(x+\gamma^2-x\gamma^2))-\Phi^{b\bar{a}}_{M^2}((1-y)(1-x)(1-\gamma^2))}{[(1-x)(1-\gamma^2)y+(x+\gamma^2-x\gamma^2)z]^2}$$

$$\times\Phi^{b\bar{c}}_{M^2_\beta}(1-y)\Phi^{c}(z'\gamma^2)G^{c\bar{a}}(z,\frac{x}{x+\gamma^2-x\gamma^2};(M^2/m^2-\frac{M^2_\beta/m^2}{(1-x)(1-\gamma^2)})(x+\gamma^2-x\gamma^2)). \qquad (21)$$

The leading contribution to $F^{ind}_{\beta\gamma}$ is due to $z'=0$, $y'=0$ and turns out to be

$$F^{ind}_{\underline{\beta}\gamma}(pq;p^{(+)}_{\beta}p^{(+)}_{\gamma}) = O(\frac{1}{s^2}) \qquad (22)$$

The same estimate (22) may also be derived for the "-" variant of the momenta. To complete the discussion we have to consider also the case b) M^2_{γ} fix , $M^2_{\beta} = \beta^2 s$. Because for both $\pm$ variants $(p_{\gamma} - q)^2 \to -\infty$, we get

$$F_{\underline{\beta}\gamma}(pq;p^{(\pm)}_{\beta}p^{(\pm)}_{\gamma}) = O(\frac{1}{s^2}). \qquad (23)$$

For $F_{\beta\underline{\gamma}}$ the role of M_{β} and M_{γ} as well as of (+) and (-) is, of course, changed. Hence, we arrive at the following contribution to W_{--}

$$W^{(iii)}_{--} \sim \frac{1}{8\pi^4 m^2}\Big(\sum_{M_{\beta}}\int_0^s dM^2_{\gamma}\frac{|F_{\underline{\beta}\gamma}(pq;p^{(+)}_{\beta}p^{(+)}_{\gamma})|^2}{\lambda^{1/2}(s,M^2_{\beta},M^2_{\gamma})} +$$

$$+\sum_{M_{\gamma}}\int_0^s dM^2_{\beta}\frac{|F_{\beta\underline{\gamma}}(pq;p^{(-)}_{\beta}p^{(-)}_{\gamma})|^2}{\lambda^{1/2}(s,M^2_{\beta},M^2_{\gamma})}\Big) \qquad (24)$$

and with eqs. (21), (B6) we obtain

$$\lim_{Bj} W(q^2,\nu) = f(x) \equiv (f^{b\bar{a}}(x) + f^{a\bar{b}}(x)), \qquad (25)$$

where

$$f^{b\bar{a}}(x) = \frac{e_c^2 m_c^2}{\pi N}(1-x)^2 \sum_{M_i^2}\int_0^1 d\rho\,(x+\rho-x\rho)^2(1-\rho)\times$$

$$\times\Big|\int_0^1 dy\int_0^1 dz\,\frac{\Phi^{b\bar{a}}_{M^2}(1-(1-z)(x+\rho-x\rho))-\Phi^{b\bar{a}}_{M^2}((1-y)(1-x)(1-\rho))}{[(1-x)(1-\rho)y+(x+\rho-x\rho)z]^2}\Phi^{c\bar{b}}_{M_i^2}(y)$$

$$\times G^{c\bar{a}}(z,\frac{x}{x+\rho-x\rho};(M^2/m^2-\frac{M_i^2/m^2}{(1-x)(1-\rho)})(x+\rho-x\rho))\Big|^2$$

and $f^{a\bar{b}}(x) = f^{\bar{b}a}(x)$ $(b \leftrightarrow a)$. (26)

The ρ-integration in (26) converges at $\rho = 0$ and 1. Moreover, the summation over M_i^2 converges since the expression under the sum is $O((\frac{1}{M_i^2})^2)$ for large M_i^2. These two convergence statements are necessary conditions for (26) to yield a finite coniribution in the Bjorken limit. In a similar way one may analyze the region $M_\beta^2 = O(\sqrt{s})$, $M_\gamma^2 = O(\sqrt{s^-})$, responsible for trajectory renormalization in the Regge limit[5]. By analogous considerations we find that the corresponding expression dies out as $q^2 \to -\infty$. Hence, the result (25) is the leading contribution of the cylinder graph in the Bjorken limit. We note that the expression (25) may dominate over the valence quarks of ref.[6] if the sea quarks are very heavy, $\frac{m_c^2}{N} >> m_a^2$, m_b^2.

To complete the discussion, we finally quote the behaviour of the structure function (25) in the limits $x \to 0$ and $x \to 1$, respectively. As in the case of the valence quarks, the behaviour of $f(x)$ at $x = 0$ turns out to be related to the Regge behaviour in just the way suggested by Abarbanel, Goldberger and Treiman[9]. With eq. (B9) we get, e.g.,

$$f^{b\bar{a}}(x) \underset{x\to 0}{=} x^{2\beta_c} \left| \frac{e_c^2 m_c^2}{\pi N} \sum_{M_i^2} \int_0^1 d\rho\, \rho^{2-2\beta_c} (1-\rho) \times \right.$$

$$\times \left| \int_0^1 dy \int_0^1 dz \, \frac{\Phi_{M^2}^{b\bar{a}}(1-\rho(1-z)) - \Phi_{M^2}^{b\bar{a}}((1-y)(1-\rho))}{[(1-\rho)\,y + \rho z]^2} \times \right.$$

$$\left. \left. \times \Phi_{M_i^2}^{c\bar{b}}(y)\, \hat{C}^{c\bar{a}}(z, (M^2/m^2 - \frac{M_i^2}{m^2(1-\rho)})\rho) \right|^2 \right| . \qquad (27)$$

Note that there is no x^{-1} behaviour being the signal of Pomeron exchange. Instead, the behaviour (27) is due

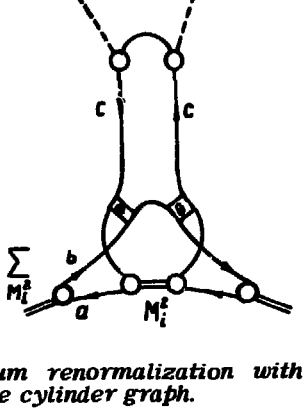

Fig. 6. Residuum renormalization with $(c\bar{c})$ *exchange obtained from the cylinder graph.*

to the exchange of an ordinary Regge trajectory ("f")with the intercept $\alpha_{c\bar{c}}(0)=-2\beta_c$ arising from the "residuum renormalization" graph shown in *fig. 6.* As β_c is a monotonously increasing function of m_c (cf. B3), we conclude that at $x=0$ the contribution of light sea quarks may dominate over the heavier valence quarks. Finally, we find from (26) using eqs. (A5, B12)

$$f^{b\bar{a}}(x) \underset{x\to 1}{\sim} A_c(1-x)^{2(\beta_a+\beta_b+\beta_c+1)} . \qquad (28)$$

Comparing eq. (28) with the valence quark behaviour [6] $\nu^2 W \underset{x\to 1}{\sim}(1-x)^{2\beta_{a,b}}$ we see that the contribution of the cylinder graph is suppressed for $x \to 1$ independent of the quark masses.

4. SUMMARY

We have investigated sea quark corrections of an order of $1/N$ to the structure function of deep inelastic scattering in QCD_2. The class of graphsconsidered con-

tains only one quark-antiquark loop and possesses the topology of the cylinder graph describing the dual bare Pomeron [7]. As our main result we find that there is no signal of a bare Pomeron in the quark partition function $f(x)$ as $x \to 0$ which is consistent with the conclusions of ref. [4,5] obtained for the Regge limit. However, to obtain this result the cancellation of different diagrams observed in the Regge limit is now unimportant. The cylinder graph yields also a finite contribution $f(x) \underset{x \to 0}{\sim} x^{-\alpha}$, α being the intercept of the exchanged "f" -trajectory, which may be interpreted as a residuum renormalization term. This expression may dominate at $x = 0$ over the valence quarks if the sea quarks are light.

It should be remarked that the absence of a bare Pomeron in QCD_2 is probably related to the lack of gluonic degrees of freedom and of gluonic bound states lying on the Pomeron trajectory.

ACKNOWLEDGEMENTS

We thank Dr. A.V.Efremov for useful discussions.

APPENDIX A

To be self-contained we list here some relevant formulas for QCD_2 needed in the text which have been discussed extensively in the literature [2,4]. The Feynman rules are *

gluon propagator: $P\frac{i}{k^2}$ (principal value)

dressed quark propagator: $$S_a(k) = \frac{i}{\not{k} - (m_a^2 - \frac{g^2 N}{\pi}) + i\epsilon} \quad \text{(A1)}$$

quark-gluon coupling: $-2ig$

---

* The gluon propagator used here differs by a factor of (-1) from that of ref. [4]. Therefore, we have also different signs in eqs. (A4) and (A6).

The normalized quark-antiquark meson vertex is defined by $(m^2 = \frac{g^2 N}{\pi})$

$$\Gamma_n^{a\bar{b}}(p,r) = -\frac{2igm}{r_-}\int_0^1 \frac{\Phi_n^{a\bar{b}}(y)}{(x-y)^2}dy; \quad x = \frac{p_-}{r_-} \qquad \text{(A2)}$$

or, if $x \in (0,1)$ and the bound state is on shell,

$$\Gamma_n(p,r) = -\frac{2ig}{mh(a,b)}\Phi_n^{a\bar{b}}(x), \qquad \text{(A3)}$$

where $\Phi_n^{a\bar{b}}(x)$ is the meson wave function of 't Hooft. The scattering matrix admits the decomposition $(x = \frac{p_-}{r_-}$, $x' = \frac{p'_-}{r_-})$

$$iT^{a\bar{b}}(p,p';r) = -\frac{4g^2 i}{r_-^2(x-x')^2} - \sum_n \frac{i}{r^2 - M_n^2}\Gamma_n^{a\bar{b}}(p,r)\Gamma_n^{a\bar{b}}(p',r). \qquad \text{(A4)}$$

It may be expressed by the Green function G,

$$G^{a\bar{b}}(x,y;\mu^2) = \sum_n \frac{\Phi_n^{a\bar{b}}(x)\Phi_n^{a\bar{b}}(y)}{\mu^2 - \mu_n^2} = G^{b\bar{a}}(1-x;1-y;\mu^2)$$
$$(\mu^2 = r^2/m^2) \qquad \text{(A5)}$$

in the following way

$$iT^{a\bar{b}}(p,p';r) = -\frac{4g^2 i}{r_-^2(x-x')^2} + \frac{4ig^2}{r_-^2}\int_0^1 dy \int_0^1 dz \frac{G^{a\bar{b}}(y,z;\frac{r^2}{m^2})}{(x-y)^2(x'-z)^2},$$

$$\text{if } x, x' \notin (0,1) \qquad \text{(A6a)}$$

$$iT^{a\bar{b}}(p,p';r) = \frac{4ig^2}{m^2 r_-}\frac{1}{h(a,b)}\int_0^1 dz \frac{G^{a\bar{b}}(x,z;\frac{r^2}{m^2})}{(x'-z)^2},$$

$$\text{if } x \in (0,1)$$
$$x' \notin (0,1) \qquad \text{(A6b)}$$

$$iT^{a\bar{b}}(p,p';r)=4ig^2\left(\frac{\delta(x-x')}{r_- m^2 h(a,b)}+\frac{G^{a\bar{b}}(x,x';\frac{r^2}{m^2})}{m^4 h(a,b)h(a',b')}\right),$$

if $x,x' \in (0,1)$. (A6c)

Finally, the quark form factor reads - $2ie_c Q^{c\bar{c}}(p,q)$,

$$Q^{c\bar{c}}(p,q)=1-\int_0^1 dy \int_0^1 dx' \frac{G^{c\bar{c}}(x',y;q^2/m^2)}{(x-x')^2}, \quad x=\frac{p_-}{-q_-} \qquad (A7)$$

or if $x \in (0,1)$

$$Q^{c\bar{c}}(p,q)=\frac{q_-}{m^2 h(c,c')}\int_0^1 G^{c\bar{c}}(x,y;\frac{q^2}{m^2})dy. \qquad (A8)$$

We have also considered a reduced G -function defined by

$$G^{a\bar{b}}(x;\mu^2)=\int_0^1 dy\, G^{a\bar{b}}(x,y;\mu^2). \qquad (A9)$$

APPENDIX B

We summarize here some properties of the functions $\Phi_n^{a\bar{b}}(x)$ and $G^{a\bar{b}}(x,y;\mu^2)$ (for details consult refs.[4, 6]).

$$\Phi_n^{a\bar{b}}(x)=(-1)^n \Phi_n^{b\bar{a}}(1-x), \qquad (B1)$$

$$\Phi_n^{a\bar{b}}(x) \underset{x\to 0}{\sim} x^{\beta_a} C^{a\bar{b}}, \qquad (B2)$$

where the power β_a is determined by

$$\frac{m_a^2}{m^2}+\pi\beta_a \cos\pi\beta_a = 1, \quad 0\le\beta_a<1. \qquad (B3)$$

Further

$$\Phi_n^{a\bar{b}}(x) \underset{n\to\infty}{\to} \sin\pi n x \qquad (B4)$$

$$\Phi_n^{a\bar{b}}\left(\frac{x}{\mu_n^2}\right) \underset{n\to\infty}{\to} \Phi^a(x); \qquad \mu_n^2 = \frac{M_n^2}{m^2} - \pi^2 n \,, \tag{B5}$$

$$\int_0^\infty dx\, \Phi^a(x) = \frac{\pi}{\sqrt{2}} \frac{m_a}{m} \,. \tag{B6}$$

The G-functions obey the following scaling relations

$$G^{a\bar{b}}\left(\frac{x}{-\mu^2}, \frac{y}{-\mu^2}; \mu^2\right) \xrightarrow[\mu^2\to-\infty]{} -\frac{1}{\pi^2}\int_0^\infty d\lambda \frac{\Phi^a(\lambda x)\Phi^a(\lambda y)}{1+\lambda}, \tag{B7}$$

$$G^{a\bar{b}}\left(\frac{x}{-\mu^2}; \mu^2\right) \xrightarrow[\mu^2\to-\infty]{} \frac{1}{\mu^2}\left(1 - \frac{\sqrt{2}\, m_a^2}{m\pi}\int_0^\infty d\lambda \frac{\Phi^a(\lambda)}{\lambda + x}\right). \tag{B8}$$

Finally, let us add some formulas not explicitly contained in the references cited. First, from (B2), (A5) we obtain

$$G^{a\bar{b}}(x, y; \mu^2) \underset{x\to 0}{\sim} x^{\beta_a} \hat{C}^{a\bar{b}}(y; \mu^2) \tag{B9}$$

$$G^{a\bar{b}}(1-x; y; \mu^2) = G^{b\bar{a}}(x, 1-y; \mu^2) \underset{x\to 0}{\sim} x^{\beta_b} \hat{C}^{b\bar{a}}(1-y; \mu^2). \tag{B10}$$

The completeness relation for the $\Phi_n^{a\bar{b}}$ yields

$$G^{a\bar{b}}(x, y; \mu^2) \underset{\mu^2\to-\infty}{\sim} \frac{1}{\mu^2}\delta(x-y) \tag{B11}$$

Using analogous techniques as those leading to eqs. (B7), (B8) we find the following additional estimates as $\mu^2 \to -\infty$ *

$$G^{a\bar{b}}\left(\frac{x}{-\mu^2}, y; \mu^2\right) = O\left(\left(\frac{1}{\mu^2}\right)^{1+\beta_a}\right), \tag{B12}$$

$$G^{a\bar{b}}\left(\frac{x}{-\mu^2}, 1-\frac{y}{-\mu^2}; \mu^2\right) = O\left(\left(\frac{1}{\mu^2}\right)^{1+\beta_a+\beta_b}\right) \,. \tag{B13}$$

---

* In ref. /4/ arguments are given in favour of $O\left(\left(\frac{1}{\mu^2}\right)^2\right)$ on the r.h.s. of (B13). We reproduce this falloff if we use the integral equation satisfied by G and (B11) under the integrals. As the approach to eq. (B11) is not uniform near $(x,y)=(0,1)$, the validity of such a behaviour is, however, not clear. Anyway, for our purposes the estimates (B12), (B13) are sufficient.

Table

	$\frac{M_\gamma^2}{s}\to 0,\ \frac{M_\beta^2}{s}\to 0$	$\frac{M_\gamma^2}{s}\to 0,\ M_\beta^2\sim\beta^2 s$	$M_\gamma^2\sim\gamma^2 s;\ \frac{M_\beta^2}{s}\to 0$	$M_\gamma^2\sim\gamma^2 s,\ M_\beta^2\sim\beta^2 s$
$p_{\beta-}$	$p_-(1-x)$ $\frac{M_\beta^2 p_-(1-x)}{s}$	$p_-(1-x)$ $\beta^2 p_-(1-x)$	$(1-\gamma^2)(1-x)p_-$ $\frac{M_\beta^2 p_-(1-x)}{s(1-\gamma^2)}$	$\frac{p_-(1-x)}{2}(1+\beta^2-\gamma^2\pm\lambda^{1/2}(1,\beta^2,\gamma^2))$
$p_{\gamma-}$	$\frac{M_\gamma^2 p_-(1-x)}{s}$ $p_-(1-x)$	$\frac{M_\gamma^2 p_-(1-x)}{s(1-\beta^2)}$ $(1-\beta^2)(1-x)p_-$	$\gamma^2 p_-(1-x)$ $p_-(1-x)$	$\frac{p_-(1-x)}{2}(1+\gamma^2-\beta^2\mp\lambda^{1/2}(1,\beta^2,\gamma^2))$
$(p-p_\beta)^2$	$(M^2-\frac{M_\beta^2}{1-x})x$ $-\frac{s}{1-x}$	$-\frac{x}{1-x}\beta^2 s$ $-\frac{s}{1-x}(1-\beta^2+\beta^2 x)$	$(M^2-\frac{M_\beta^2}{(1-\gamma^2)(1-x)})(x+\gamma^2-x\gamma^2)$ $-\frac{s(1-\gamma^2)}{1-x}$	$s\frac{\beta^2+\gamma^2-2\beta^2 x-1\pm\lambda^{1/2}(1,\beta^2,\gamma^2)}{2(1-x)}$
η	$\frac{x}{1-x}$ $\frac{s}{M_\beta^2(1-x)}$	$\frac{x}{1-x}$ $\frac{1}{\beta^2(1-x)}-1$	$\frac{1}{(1-\gamma^2)(1-x)}-1$ $\frac{s}{M_\beta^2}\frac{1-\gamma^2}{1-x}$	$\frac{2}{(1-x)(1+\beta^2-\gamma^2\pm\lambda^{1/2}(1,\beta^2,\gamma^2))}-1$
η'	$\frac{M_\gamma^2(1-x)}{xs}$ $\frac{1-x}{x}$	$\frac{M_\gamma^2(1-x)}{xs(1-\beta^2)}$ $\frac{(1-\beta^2)(1-x)}{x}$	$\gamma^2\frac{1-x}{x}$ $\frac{1-x}{x}$	$\frac{1-x}{2x}(1+\gamma^2-\beta^2\mp\lambda^{1/2}(1,\beta^2,\gamma^2))$

REFERENCES

1. *Gross D.J., Wilczek F. Phys. Rev., 1973, D8, p.3633; ibid., 1974, D9, p.980. Politzer H.D. Phys.Rep., 1974, 14, p.129.*
2. *"t Hooft G. Nucl.Phys., 1974, B72, p.461. Callan C.G. Jr., Coote N., Gross D.J. Phys.Rev., 1976, D13, p.1649. Marinov M.S., Perelomov A.M., Terent'ev M.V. JETP. Lett., 1974, 20, p.225.*
3. *Ebert D., Pervushin V.N. JINR, E2-10730, Dubna, 1977; ibid., E2-10731, Dubna, 1977.*
4. *Brower R.C. et al. Phys.Lett., 1976, 65B, p.249 and CERN Preprints TH 2283, 2295, 1977; Ellis J. Applications of QCD (Zakopane Lectures), 1977.*
5. *Einhorn M.B., Nussinov S., Rabinovici E. Michigan prepr., UM HE, 1976, 76-39. Einhorn M.B., Rabinovici E. Nucl.Phys., 1977, B128, p.421.*
6. *Einhorn M.B. Phys.Rev., 1976, D14, p.3451.*
7. *"Dual Theory" - ed. by M.Jacob (North-Holland, Amsterdam, 1974); Ebert D., Otto H.J. A Survey on Dual Tree and Loop Amplitudes. Fortschr. d. Phys., 1977, 25, p.203.*
8. *Kripfganz J., Schmidt M.G. Nucl.Phys., 1977, B125, p.323.*
9. *Abarbanel H.D.J., Goldberger M.L., Treiman S.B. Phys.Rev.Lett., 1969, 22, p.500.*

Received by Publishing Department on December 30, 1977.

SUBJECT CATEGORIES

OF THE JINR PUBLICATIONS

Index	Subject
1.	High energy experimental physics
2.	High energy theoretical physics
3.	Low energy experimental physics
4.	Low energy theoretical physics
5.	Mathematics
6.	Nuclear spectroscopy and radiochemistry
7.	Heavy ion physics
8.	Cryogenics
9.	Accelerators
10.	Automatization of data processing
11.	Computing mathematics and technique
12.	Chemistry
13.	Experimental techniques and methods
14.	Solid state physics. Liquids
15.	Experimental physics of nuclear reactions at low energies
16.	Health physics. Shieldings
17.	Theory of condensed matter

Издательский отдел Объединенного института ядерных исследований.
Заказ 24336. Тираж 650. Уч.-изд. листов 1,51.
Редактор Э.В. Ивашкевич. Подписано к печати 30.01.78 г.
Корректор Р.Д. Фомина.